AD_____

Award Number: W81XWH-09-1-0127

TITLE: The Role of the Omental Microenvironment in Ovarian Cancer Metastatic Colonization

PRINCIPAL INVESTIGATOR: Carrie W. Rinker-Schaeffer, Ph.D.

CONTRACTING ORGANIZATION: The University of Chicago
Chicago, IL 60637

REPORT DATE: August 2012

TYPE OF REPORT: Annual

PREPARED FOR: U.S. Army Medical Research and Materiel Command
Fort Detrick, Maryland 21702-5012

REPORT DOCUMENTATION PAGE

Form Approved
OMB No. 0704-0188

1. REPORT DATE	2. REPORT TYPE	3. DATES COVERED
August 2012	Annual	1 Aug 2011 – 31 Jul 2012

4. TITLE AND SUBTITLE

The Role of the Omental Microenvironment in Ovarian Cancer Metastatic Colonization

5a. CONTRACT NUMBER

5b. GRANT NUMBER
W81XWH-09-1-0127

5c. PROGRAM ELEMENT NUMBER

6. AUTHOR(S)

Carrie Rinker-Schaeffer, Ph.D., Robert Clark, B.S., and Venkat Krishnan, Ph.D.

E-Mail: crinkers@uchicago.edu

5d. PROJECT NUMBER

5e. TASK NUMBER

5f. WORK UNIT NUMBER

7. PERFORMING ORGANIZATION NAME(S) AND ADDRESS(ES)
The University of Chicago
Chicago, IL 60422

8. PERFORMING ORGANIZATION REPORT NUMBER

9. SPONSORING / MONITORING AGENCY NAME(S) AND ADDRESS(ES)
U.S. Army Medical Research and Materiel Command
Fort Detrick, Maryland 21702-5012

10. SPONSOR/MONITOR'S ACRONYM(S)

11. SPONSOR/MONITOR'S REPORT NUMBER(S)

12. DISTRIBUTION / AVAILABILITY STATEMENT
Approved for Public Release; Distribution Unlimited

13. SUPPLEMENTARY NOTES

14. ABSTRACT

In order to control ovarian cancer metastasis formation, there is significant interest in identifying the tissue microenvironments involved in cancer cell colonization of the omentum. Omental adipose is a site of prodigious metastasis in both ovarian cancer models and clinical disease. It is unusual as it contains milky spots, structures consisting of immune cells, stromal cells and structural elements surrounding glomerulus-like capillary beds. Contrary to studies reporting that omental colonization is adipocyte-driven, work presented herein shows that milky spots and adipocytes play distinct, complementary roles in omental metastatic colonization. Specifically, *in vivo* assays showed that ID8, CaOV3, HeyA8 and SKOV3ip.1 cancer cells preferentially lodge and grow within omental and splenoportal fat, which contain milky spots, as compared to other peritoneal fat depots. Similarly, media conditioned by milky spot-containing adipose tissue caused 75% more cell migration than media conditioned by milky spot-deficient adipose. Studies using a panel of immune-deficient mice showed that the mouse genetic background does not alter omental milky spot number and size, nor does it affect ovarian cancer colonization. Finally, consistent with the role for lipids as an energy source for cancer cell growth, *in vivo* time-course studies found an inverse relationship between metastatic burden and omental adipocyte content. Our findings provide new insights into the critical role milky spots play in omental metastatic colonization, the critical first step in the development of widespread peritoneal disease.

15. SUBJECT TERMS

Nothing Listed

16. SECURITY CLASSIFICATION OF:			17. LIMITATION OF ABSTRACT	18. NUMBER OF PAGES	19a. NAME OF RESPONSIBLE PERSON
a. REPORT	b. ABSTRACT	c. THIS PAGE			USAMRMC
U	U	U	UU	70	19b. TELEPHONE NUMBER *(include area code)*

Table of Contents

Introduction: In order to more clearly define the functional role of milky spots and their components in metastatic colonization, we evaluated the lodging and progressive growth of ovarian cancer cells in peritoneal fat that either contains or lacks milky spots. *In vivo* studies using a panel of ovarian cancer cell lines showed that milky spots dramatically enhance early cancer cell lodging on peritoneal adipose tissues. Similarly, conditioned medium from milky spot-containing fat had a significantly increased ability to direct cell migration, compared with conditioned medium from milky spot-deficient fat. Studies using a panel of immunodeficient mice showed that the number and size of omental milky spots is not dependent on the mouse genetic background and, similarly, that ovarian cancer cell colonization does not depend on the immune composition of the milky spot. Finally, consistent with the role for lipids as an energy source for ovarian cancer cell growth, *in vivo* time-course studies revealed an inverse relationship between metastatic burden and omental adipocyte content.

Body: After escape from the primary tumor, ovarian cancer cells in the peritoneal fluid have access to and can potentially lodge within a variety of tissues (1,2). In both clinical disease and experimental models, however, the omentum is the site of prodigious metastasis formation (3-5). Thus, attachment of ovarian cancer cells to the omentum represents an early step in the development of widespread peritoneal disease (6,7). As the central regulator of peritoneal homeostasis, its functions include regulating fluid and solute transport, sensing and repairing injuries, promoting angiogenesis, fighting infection, serving as a source of stem cells, producing regulatory molecules, and storing and supplying lipids (8-12). These diverse functions are conferred by the cellular composition and architecture characteristic of human omenta.

Aside from the clear collagenous membrane that acts as a scaffold for the organ, the majority of the omentum is composed of bands of adipose tissue that contain adipocytes, blood and lymph vessels, immune cells, stromal cells, and connective matrix components that lie beneath an irregular mesothelium (8-12). In general, adipocytes have a variety of functions, ranging from lipid storage to production of endocrine molecules, and can serve as an integrating hub for inflammation, metabolism, and immunity (13-20). A distinctive feature of the omental vasculature is the presence of numerous branching blood vessels ending in tortuous glomerulus-like capillary beds near the tissue periphery (21-23). Immune cells aggregate around and within these capillary beds to form milky spots, which are the major immune structure for host defense of the peritoneal cavity (20, 25-36). In milky spots, both the endothelial lining of the capillaries and the overlying mesothelium are specially adapted to facilitate transmigration of immune cells (35). Additional structural elements include plasmocytes, fibroblasts, and mesenchymal cells, as well as collagen and reticular and elastic fibers (21).

A comprehensive literature review showed that studies examining the role of the omentum in metastasis focus on the contribution of its individual components, and not on the tissue as a whole. In our view, results from the majority of studies support models in which ovarian cancer metastatic colonization is driven either purely by milky spots or purely by adipocytes. The milky spot-driven model is based on a large body of *in vivo* data showing that, on intraperitoneal injection, cancer cells rapidly and specifically localize, invade, and proliferate within omental milky spots (36-40). In contrast, the adipocyte-driven model is based on studies published since the awarding of this grant. This model was prompted by the observation that, in its resting state, the omentum is composed predominantly of adipose and that cultured adipocytes can produce adipokines capable of promoting ovarian cancer cell migration and invasion *in vitro* (41). Adipocytes can also provide a proliferative advantage by transferring fatty acids to ovarian cancer cells (41). Although both models have clear strengths, neither addresses the intimate and dynamic interaction among milky spots, surrounding adipocytes, and other components of omental tissues.

Key Research Accomplishments:

1. Identified both milky spot containing and deficient depots of peritoneal adipose to use to dissect that role(s) of milky spots and adipocytes in the promotion of ovarian cancer cell metastatic colonization.
2. Ovarian cancer cells preferentially colonize peritoneal adipose that contains milky spots.
3. Omental tissues secrete a factor(s) that can promote ovarian cancer cell migration.
4. Milky spot-containing tissues show enhanced ability to stimulate directed migration.
5. *In vivo* colonization of omental milky spots by ovarian cancer cells is not dependent on their immune cell composition.
6. During progressive growth ovarian cancer cells replace omental adipose.

Reportable Outcomes:

Several sources of adipose tissue are accessible to ovarian cancer cells in the peritoneal cavity. There are five major adipose depots structures in the peritoneal cavity (2). As shown in Figure 1A, a lateral view of a ventral dissection allows visualization of the omentum (OM), gonadal fat (GF), uterine fat (UF), and mesentery (MY). The ovary (ov), uterine horn (uh) and small intestine (si) are indicated as points of reference. Further dissection allows for clear visualization of the splenoportal fat (SP), which surrounds the splenic artery and connects the hilum of the spleen to the celiac artery (Figure 1B), and the omentum, shown isolated from the pancreas (Figure 1C). The gross structure and relative size of these tissues is shown in Figure 1D.

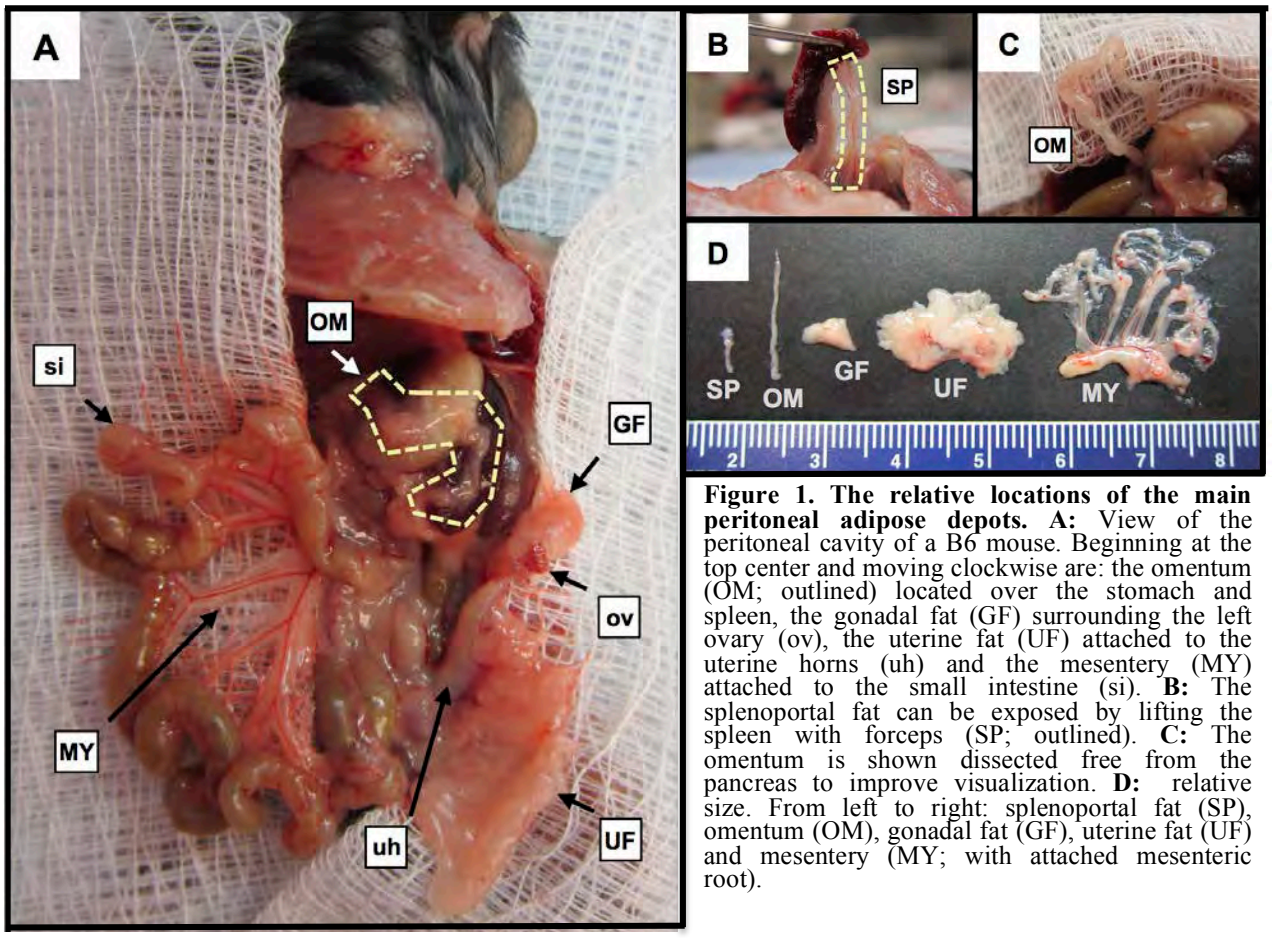

Figure 1. The relative locations of the main peritoneal adipose depots. A: View of the peritoneal cavity of a B6 mouse. Beginning at the top center and moving clockwise are: the omentum (OM; outlined) located over the stomach and spleen, the gonadal fat (GF) surrounding the left ovary (ov), the uterine fat (UF) attached to the uterine horns (uh) and the mesentery (MY) attached to the small intestine (si). **B:** The splenoportal fat can be exposed by lifting the spleen with forceps (SP; outlined). **C:** The omentum is shown dissected free from the pancreas to improve visualization. **D:** relative size. From left to right: splenoportal fat (SP), omentum (OM), gonadal fat (GF), uterine fat (UF) and mesentery (MY; with attached mesenteric root).

Interestingly, in 1995 Takemori *et al*, reported the presence of milky spots in the splenoportal fat of New Zealand Black mice that are similar in structure and composition to omental milky spots; however, they did not examine cancer cell localization to these structures (42). Consistent with their findings, we found that both the omentum and splenoportal fat have archetypal milky spot structures (Figure 2A). In contrast, these structures were not observed in uterine, gonadal and mesenteric fat (Figure 2A). Further, 7 days after i.p. injection of SKOV3ip.1 cells, comparable cancer cell lesions were observed in both omental and splenoportal fat (Figure 2B) and not other fat depots. IHC using a human pan-cytokeratin (pan-CK) antibody showed that the lesions were composed of SKOV3ip.1) cells intermingled with the immune cells. The specificity of IHC staining was confirmed by staining with an IgG control antibody (Figure 2B).

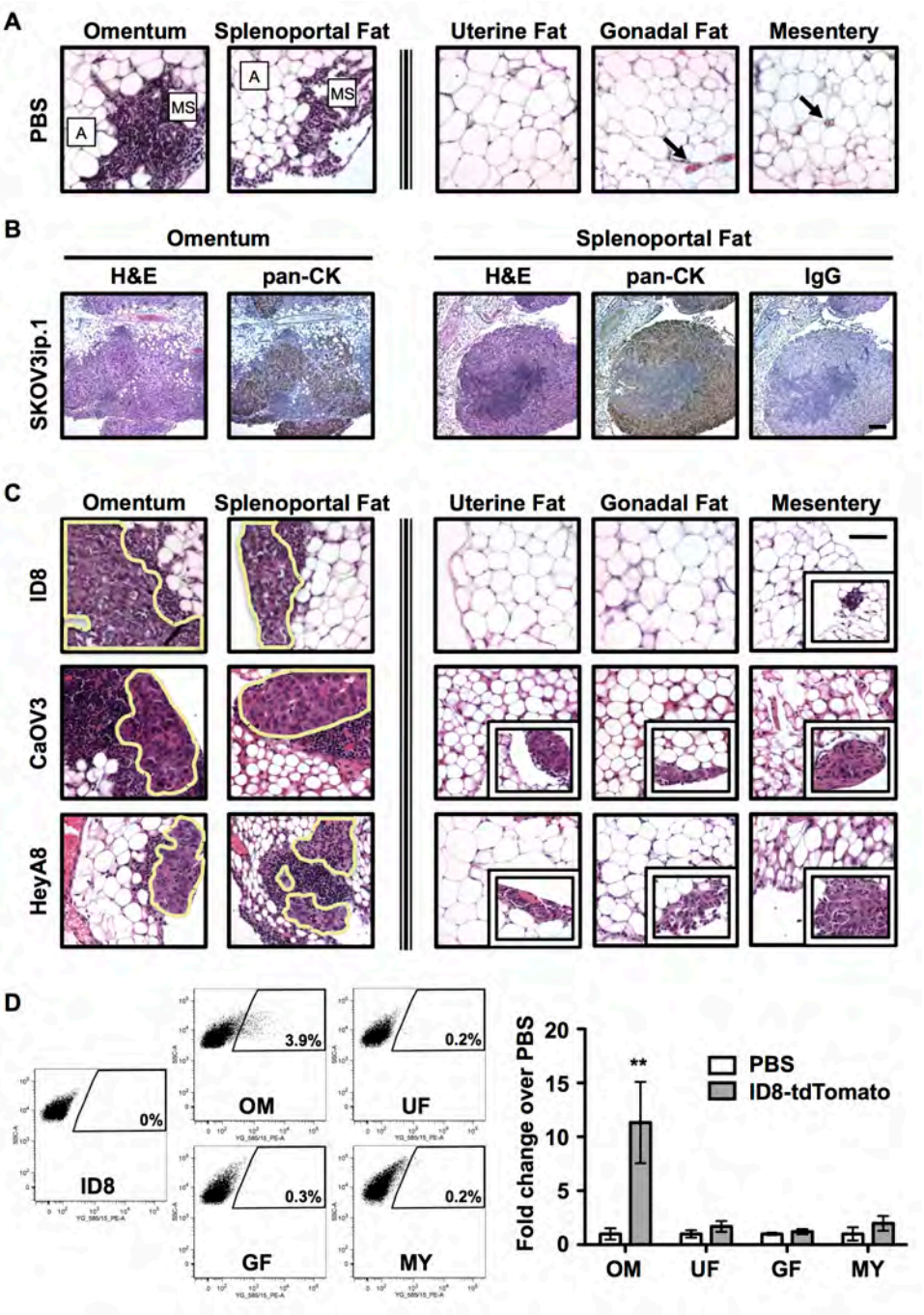

Figure 2. Ovarian cancer cells preferentially colonize peritoneal adipose that contains milky spots. A: Milky spots (MS) are observed in the adipose (A) of the omentum and splenoportal fat of PBS-injected and naïve mice. In contrast, no milky spots were detected in the uterine fat, gonadal fat and mesentery, each composed mostly of adipocytes. Representative data from PBS-injected B6 mice is shown. *Arrows* indicate blood vessels. Scale bar equals 50 μm. **B.** Standard histology and IHC shows comparable colonization of milky spots in both omentum and splenoportal fat (after injection of $1x10^6$ SKOV3ip.1 cells into Nude mice). Sections evaluated by H&E staining. Epithelial (cancer) cells within the lesions were confirmed by IHC for cytokeratin using a pan-cytokeratin (pan-CK) antibody. IHC using an IgG isotype antibody for pan-cytokeratin served as a control. The scale bar is the same for all images and denotes 100 μm. **C.** Eval-uation of ID8, CaOV3, and HeyA8 ovarian cancer colonization of peritoneal fat depots at 7 dpi. Cancer cell lesions are outlined. Representative exam-ples of the cancer lesions occasionally seen in uterine, gonadal, and mesenteric fat are shown in insets. **D.** Flow cytometric analyses of omentum (OM), uterine fat (UF), gonadal fat (GF), and mesentery (MY) harvested from mice at 7 dpi of ID8-tdTomato cells. Data is presented as fold change increase of tdTomato-postive cells over PBS-injected mice (right). Error bars indicate standard error of the mean. ** denotes $p<0.01$ compared to PBS controls.

Ovarian cancer cells preferentially colonize peritoneal adipose that contains milky spots. As described in the introduction, a review of the literature showed that ovarian cancer's predilection for omental metastasis formation can be ascribed to either adipose-driven or milky spot-driven mechanisms. However, these models are based upon studies focusing on either structural features (i.e. milky spots) or cellular components (i.e. adipocytes) of omental tissue (25,38,41). The availability of peritoneal fat depots that contain or lack milky spot structures enabled us to distinguish experimentally between the two models in the physiologically relevant setting of the peritoneal cavity. We reasoned that if colonization were purely adipocyte-driven, ovarian cancer cells would colonize the various peritoneal adipose depots to a similar extent after i.p. injection. In contrast, if milky spots drive this process, the omentum and splenoportal fat would have cancer cell foci in their numerous milky spots, while uterine, gonadal, and mesenteric fat would essentially be free of cancer cell colonies. Although our previous studies using SKOV3ip.1 cells support this latter model, studies using additional ovarian cancer cell lines are needed to determine the generalizability of these findings. To this end, the ability of ID8, CaOV3, and HeyA8 cells to form cancer cell foci on the five distinct peritoneal fat after i.p. injection into B6 (ID8) or Nude (CaOV3, HeyA8) mice was assessed by histology. The average number of cancer cells in a representative section of tissue was determined and expressed as foci/slide (Table 1). At 7 dpi, numerous large foci of ID8 cells were seen within the milky spots of both the omentum (ave. 48 foci/slide) and splenoportal fat (ave. 5 foci/slide) (Figure 2C). No ovarian cancer cells were detected in the uterine or gonadal fat (Figure 2C). In the mesentery, small clusters (<10 cells) of cancer cells were seen observed (ave. 2 foci/slide) on the tissue periphery (Figure 2C, *inset*). In agreement with these findings, CaOV3 cells showed similar pattern and extent of foci formation in the peritoneal adipose (Figure 2C*, inset*). Interestingly, HEYA8 cells had a greater ability to form surface foci on gonadal fat (UF) with 8 foci/slide (ave). [Figure 2C, *inset* (Table 1)].

Table 1. Histologic assessment of ID8, CAOV3, and HeyA8 colonization of peritoneal adipose depots

Mouse Strain	Cell Line	Tissue Type	Presence of Cancer Foci in Adipose Depot[a]	# Foci/Slide	Ave. # Foci/ Slide
C57Bl/6	ID8	OM	5 / 5	36, 46, 50, 51, 58	48
		SP	5 / 5	3, 3, 6, 6, 6	5
		GF	0 / 5	0, 0, 0, 0, 0	0
		MY	5 / 5	1, 1, 1, 2, 4	2
		UF	0 / 5	0, 0, 0, 0, 0	0
Nude	CaOV3	OM	5 / 5	17, 19, 22, 23, 24	21
		SP	5 / 5	7, 7, 13, 13, 20	12
		GF	1 / 5	1, 0, 0, 0, 0	0
		MY	5 / 5	1, 2, 2, 4, 4	3
		UF	2 / 5	1, 1, 0, 0, 0	0
	HeyA8[b]	OM	4 / 4	25, 27, 29, 35	29
		SP	4 / 4	6, 7, 8, 10	8
		GF	3 / 4	1, 1, 3, 0	1
		MY	4 / 4	1, 4, 6, 8	5
		UF	4 / 4	6, 6, 10, 11	8

[a] Incidence of cancer foci in organ in each of 5 mice injected
[b] HeyA8 mouse cohort n=4 due to mis-injection of an individual mouse

Finally, to complement our findings from our histological analyses and enable future studies, we developed a protocol to quantitate the number of cancer cells present in peritoneal adipose depots. ID8-tdTomato cells were prepared and injected i.p. into B6 mice. At 7 dpi, the adipose organs were harvested and dissociated into a single-cell suspension. The number of tdTomato cells present in the population of remaining cells (i.e. immune, endothelial, and mesothelial cells, fibroblasts, etc.) was quantified via flow cytometry as described in the Materials and Methods. It should be noted that splenoportal fat was excluded because its small size prohibited reliable cell recovery. As shown in Figure 2D, omental tissue preparations contained a significant population of tdTomato-positive cells. When quantified (Figure 2D, *right*), the omentum showed a ~ 12-fold increase in the number of ID8-tdTomato cells present over PBS-injected controls while there was no significant increase in cell preps

from the gonadal fat, uterine fat, or mesentery. These data support our histological finding that ovarian cancer cells preferentially colonize milky spot-containing adipose and provide an additional quantitative method for future studies by our laboratory and others.

Omental tissues secrete a factor(s) that can promote ovarian cancer cell migration. Ovarian cancer cells specifically localize to the omentum within minutes after i.p. injection (3, 6, 36). This suggests that omental tissue produces a factor(s) that promotes cancer cell homing; however, previous studies have only examined the contribution of isolated adipocytes (41). To address this gap in knowledge, we first tested the ability of omentum-conditioned media to promote directed cancer cell migration. Using a modification of our published method for *ex vivo* organ culture (6), omenta were excised and allowed to normalize in DMEM/F12 media containing 20% FCS for 24 hrs. Tissues were then rinsed with PBS, placed in serum-free DMEM/F12, and maintained for up to 5 days *ex vivo*. Tissue integrity was assessed both histologically by visually evaluating intact (round, continuous cell membrane) versus necrotic (stellate, discontinuous cell membrane) adipocytes and functionally by measuring the level of IL-6 in the conditioned media every 24 hrs. In agreement with our previously published studies (6), omental tissues did not show loss of integrity or function under these conditions (Figure 3).

After normalization in DMEM/F12 containing 20% FCS, omenta were rinsed with PBS and allowed to condition serum-free DMEM/F12 for 24 hrs (subsequently referred to as conditioned serum-free media; CSF). Omenta maintained in serum-free (SF) media are termed starved omenta (SOM). The combinations of omenta and media used as chemoattractants for the 6 hr migration assay are summarized in Figure 4A, upper panel, while representative membranes from the migration assays are shown in Figure 4A, lower panel. The number of cells that migrated to the lower side of the membrane was determined by summing the number of cells in each of 5 independent fields observed at 100x magnification.

Initial studies tested the ability of omenta harvested from CD1 mice to promote migration of both mouse ID8 and human SKOV3ip.1 cells (Figure 4B). CD1 CSF media served as a strong chemoattractant for both ID8 and SKOV3ip.1 cells, resulting in a greater than 150-fold increase in migration relative to SF media controls. To ensure that these results are not specific to omenta harvested from CD1 mice, CSF from B6 and Nude mouse omenta were also tested in their ability to promote ID8 and SKOV3ip.1 cell migration. As shown in Figure 4C, CSF prepared from B6 and Nude mouse omenta were a strong chemoattractant for ID8 cells, stimulating migration on a par with CD1-conditioned media (Figure 4B). Consistent with this finding, B6 and Nude CSF also stimulated equivalent levels of migration in SKOV3ip.1 cells. Interestingly, SKOV3ip.1 cells show a consistently lower level of migration than ID8 cells in response to media conditioned by omenta from CD1, B6, and Nude mice. Taken together, these experiments showed that intact omental tissue can be used as a starting point for efforts to identify one or more secreted factors that promote ovarian cancer cell homing to omental tissues.

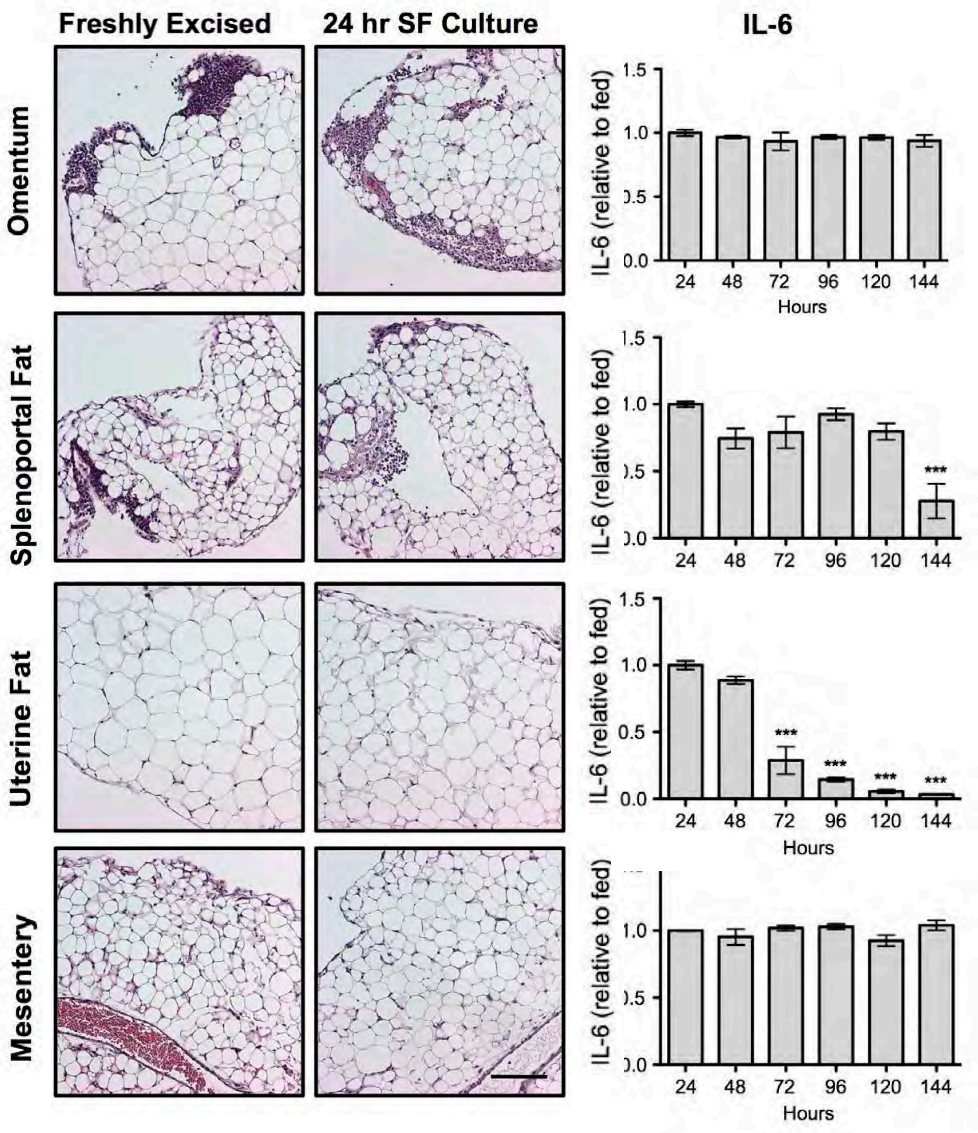

Figure 3. Evaluation of tissue integrity and function of tissues maintained in *ex vivo* culture. Left column: The appearance of freshly excised tissues. **Middle column:** Histology of tissues maintained for 24 hr in serum-free DMEM/F12. **Right column:** To assess tissue viability and function under *ex vivo* conditions, the amount of IL-6 in the SF culture media was determined at 24 hr intervals. As a control, the amount of IL-6 secreted by tissues maintained in media containing 20% FCS was determined in parallel. The relative amount of IL-6 at each timepoint is the ratio of the measured IL-6 concentration to the IL-6 concentration in the control group. The scale bar is the same for all images and denotes 50 μm. Error bars indicate standard error of the mean, *** denotes $p<0.001$.

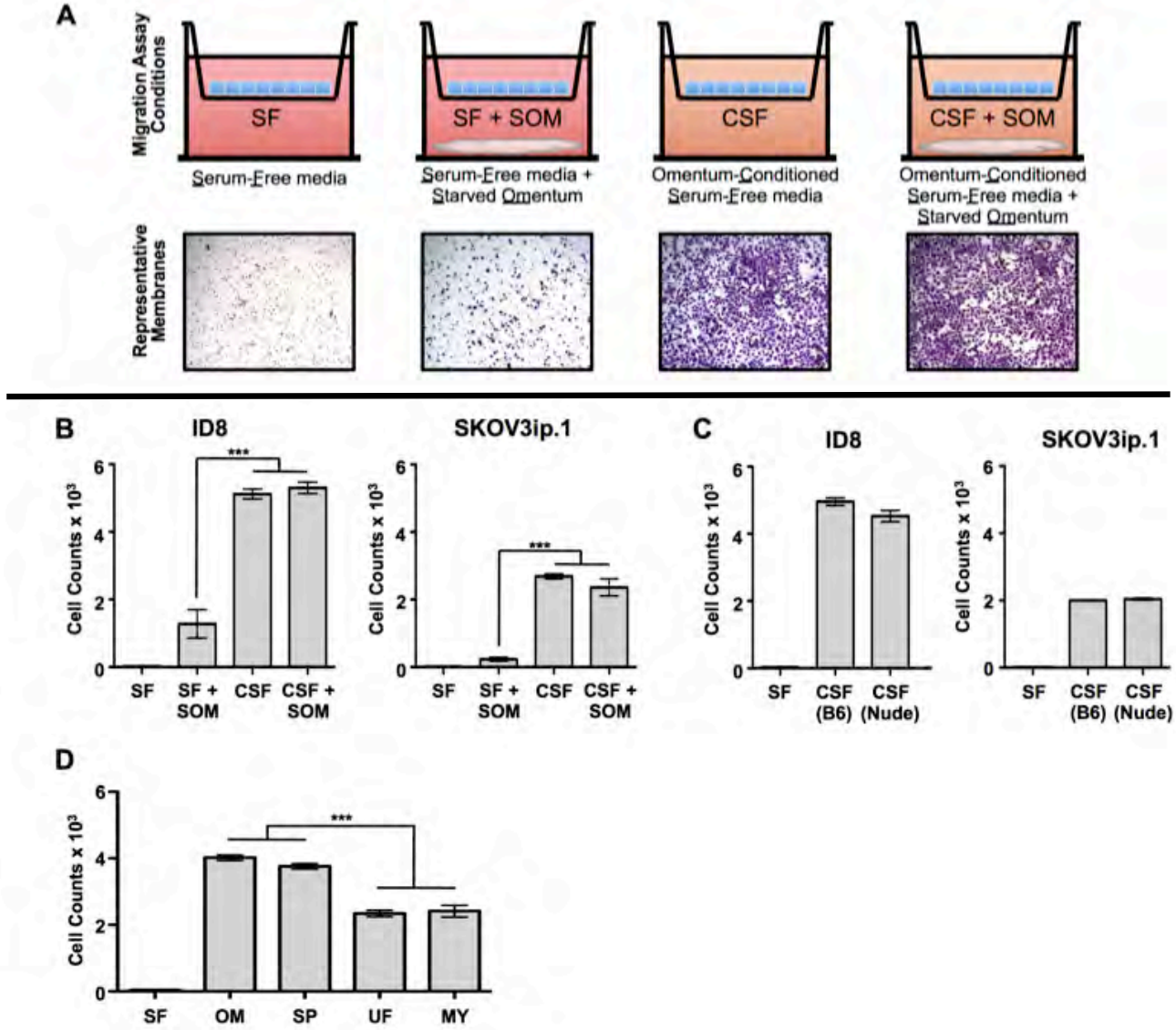

Figure 4. Milky spot-containing adipose tissues show enhanced ability to stimulate directed migration. A: *Top:* Depiction of migration assay setup. Cancer cells are placed in the upper chamber of the transwell apparatus. The chemoattractant media, with or without starved tissue, is placed in the lower chamber as indicated. *Bottom:* Representative membranes from ID8 migration assays. **B:** Quantitation of ID8 (*left*) and SKOV3ip.1 (*right*) cell migration in response to factors produced by omenta harvested from CD1 mice. Conditions are those illustrated in Panel A, where SF denotes serum free media where CSF denotes conditioned serum and SOM denotes starved omentum. **C:** Quantitation of ID8 (*left*) and SKOV3ip.1 (*right*) cell migration in response to media conditioned by omenta from either B6 or Nude mice [indicated as CSF(B6) and CSF(Nude), respectively]. **D:** Migration assay of ID8 cells toward serum-free media conditioned for 24 hr by tissue equivalents of omenta (OM), splenoportal fat (SP), uterine fat (UF) and mesentery (MY) harvested from B6 mice. n=5 for all conditions. Error bars indicate standard error of the mean, *** denotes $p<0.001$.

Milky spot-containing tissues show enhanced ability to stimulate directed migration. In their work, Nieman *et al*. showed that adipocytes cultured *in vitro* secreted cytokines that can promote migration of SKOV3ip.1 ovarian cancer cells (41). This raised the possibility that migration of cancer cells toward omentum-conditioned media could be a strictly adipose-driven process. If that were the case, we predicted that media conditioned by adipose tissue lacking milky spots would promote migration of ovarian cancer cells to the same extent as milky spot-containing adipose tissue. Alternatively, if milky spots play a key role in organ-specific homing, we expected that conditioned media from tissues containing milky spots could have an enhanced ability to promote migration. To distinguish between these possibilities, CSF media was prepared using weight-matched tissue equivalents of omentum, splenoportal fat, uterine fat, and mesentery and used as a chemoattractant in transwell migration assays. As shown in

Figure 3 tissues did not show loss of integrity or function for the duration of the migration assay. However, it was noted that the IL-6 production of the cultured uterine fat dropped significantly at 3 days in culture (Figure 3). The migration-promoting activity of CSF prepared from each of these tissues is summarized in Figure 4D. Media conditioned by omenta and splenoportal fat caused a 95-fold increase in cell migration as compared to SF media controls. In contrast, the absence of milky spots in uterine fat and mesentery corresponded with 75% reduction in the migration-stimulatory activity in their conditioned media (Figure 4D). Taken together, these functional studies bridge the adipocyte-driven and milky spot-driven models and argue that the presence of milky spots increases the chemoattractive potential of peritoneal fat depots.

***In vivo* colonization of omental milky spots by ovarian cancer cells is not dependent on their immune cell composition.** As a first step toward understanding the effect of the immune cell composition of milky spot structures on ovarian cancer cell colonization, experimental metastasis assays were conducted using immune competent (B6) and immunodeficient (Igh6, Nude, Rag1, and BN XID) mice. Specifically, 1 x 10^6 ID8 ovarian cancer cells were injected i.p. into all of the 5 different mouse strains. Cancer cell foci were observed within milky spots in each of these mouse strains at 7 dpi (Figure 5A) and were confirmed to be epithelial via positive staining for mouse cytokeratin 8/18 (CK8/18). To determine if the missing immune-cell types in the various immune-deficient mice alters cancer localization to milky spots, DAB area was quantified in CK8/18 stained sections. Figure 5B shows that ID8 cancer cells colonize omenta from each strain to a statistically equivalent degree. In parallel, 1 x 10^6 SKOV3ip.1 human ovarian cancer cells were injected into Nude, Rag1, and BN XID mice, and cancer foci were again found in each mouse strain (Figure 5C). SKOV3ip.1 lesions were stained for human pan-cytokeratin (pan-CK) and found to be cytokeratin-positive. Thus, ovarian cancer cell colonization of omental milky spots is not affected by deficiency or absence of T cells, B cells and/or NK cells in these mouse strains.

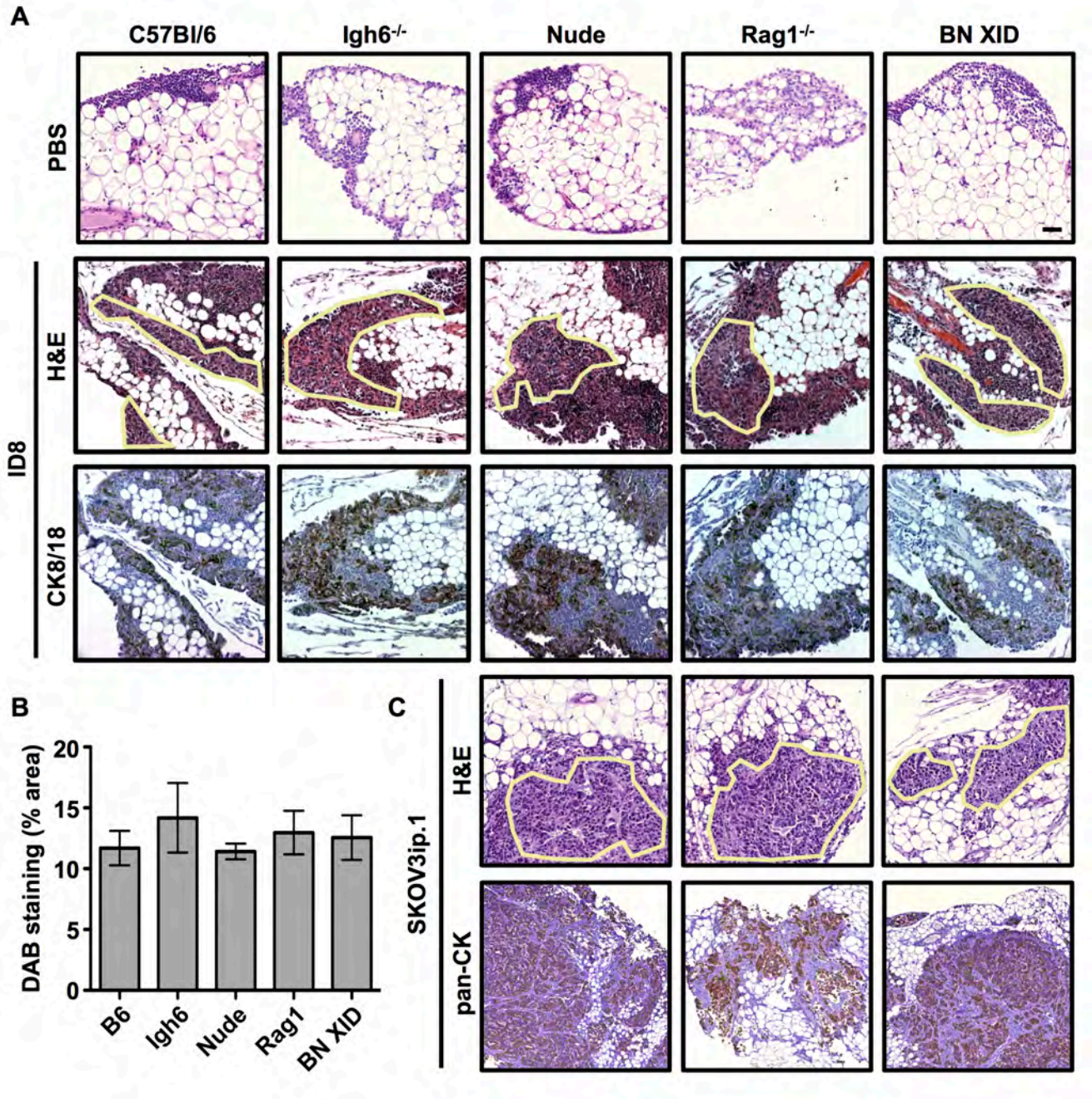

Figure 5. Colonization of omental milky spots by ovarian cancer cells is not dependent on the host immune status. To test the possibility that the immune composition of the milky spots has a quantitative effect on ovarian cancer cell colonization, mice with deficiencies in T cells, B cells and/or NK cells were injected i.p. with either PBS (control) or $1x10^6$ ovarian cancer cells. **A:** B6, Igh6$^{-/-}$, Nude, Rag1$^{-/-}$ and BN XID mice were injected with mouse ID8 cells (syngeneic to B6 background). Omenta were collected at 7 dpi and stained with H&E. Cancer cell foci within milky spots are outlined. IHC against mouse cytokeratin 8/18 (CK8/18) was used to confirm that the epithelial origin of the cancer cell foci. **B:** DAB staining area is used as an indicator of cancer cell burden in omental tissues. Values calculated as the percentage of ID8 with strong and medium intensity of CK8/18 (DAB) staining normalized to total stained area of the slide. Error bars indicate standard error of the mean. **C:** Human SKOV3ip.1 cells were injected into Nude, Rag1$^{-/-}$ and BN XID mice and treated similarly to ID8 injected animals. IHC for against human pan-cytokeratin (pan-CK) was used to confirm the epithelial origin of cancer cell lesions. Samples from 5 independent animals were evaluated for each condition of each test. The scale bar is the same for all images and denotes 50 μm.

During progressive growth ovarian cancer cells replace omental adipose. Mechanistic studies by Nieman *et al*. indicated that ovarian cancer cells could use adipocytes as an energy source for tumor growth (41). If this holds true *in vivo*, we predicted that as cancer cells proliferate, they interact with and consume adipocyte lipids. The ultimate outcome of this inverse relationship between cancer cell area and adipocyte area would be that, at the experimental endpoint, the omental adipose would be replaced completely with cancerous tissue. To test this notion, 1 x 10^6 ID8 ovarian cancer cells were injected i.p. into a cohort of B6 mice. Groups of 5 mice were euthanized and tissues collected for histologic analysis at 1, 3, 6 and 9 weeks post injection (Figure 6A). Consistent with an inverse relationship between ovarian cancer cell growth and adipocyte depletion, there is a marked reduction in the adipocyte area over time. To quantify this change, we used a pixel-based image processing protocol similar to milky spot quantification (detailed in the Materials and Methods) to calculate the adipocyte area in omenta over time. This showed a linear decrease in the percentage of adipocytes in the omentum corresponded to the expansion of ID8 cancer cell lesions (Figure 6B). These data are consistent with cancer cells' utilization of lipids stored in adipocytes as an energy source for their continued growth.

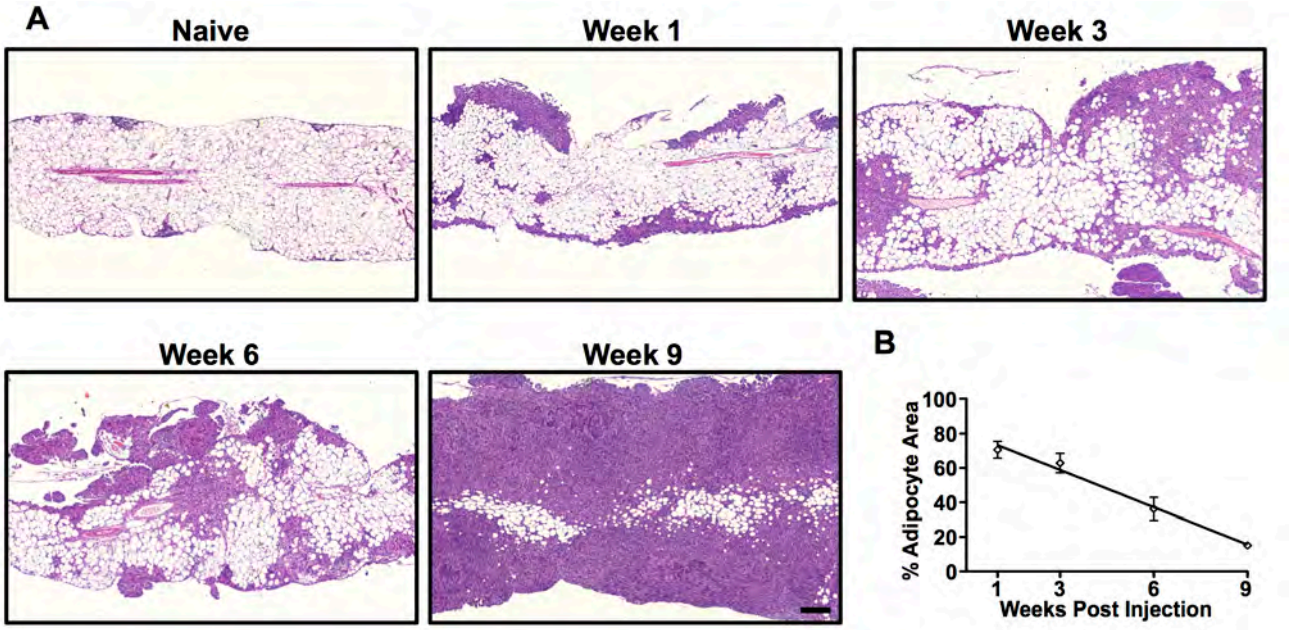

Figure 6. Adipocyte area of the omentum decreases during the timecourse ovarian cancer growth. A: The first panel shows a representative H&E stained section of an omentum from a naive B6 mouse. Milky spots are seen within adipose at the tissue periphery. The four subsequent panels show representative images of omental tissues harvested from B6 mice at 1, 3, 6 and 9 weeks post injection. The scale bar is the same for all images and denotes 200 μm. **B:** Quantitation of adipocyte area from H&E images. Reported values are percent adipocyte area normalized to whole omental area. Data at each time point is based on five independent animals. Error bars indicate standard error of the mean. A linear regression of the data points indicates a slope significantly deviant from zero ($p<0.0001$) with $R^2 = 0.8145$.

Conclusions and Future Directions:

There is now considerable literature on the structure and function of milky spots in both the omentum and extraomental sites. Beginning in the 1970s, investigators noted that ascites tumors had a proclivity for these structures (42). Subsequent studies have confirmed and refined these findings (3, 6, 36). The strength of this work is that it implies a functional role for milky spots in the early steps of omental colonization. However, the weakness of the "milky spot-driven" model prompted by this body of literature is that the studies on which it is based do not consider the potential contribution(s) of adipocytes and other cells within the omentum. While the failure to consider the contribution of

omental adipose in cancer metastasis is consistent with the now-antiquated view of adipocytes as an inert component of connective tissues (13, 18, 19), it is a fundamental oversight that must be addressed if we are to understand the organ specificity of ovarian cancer cells.

In contrast, the adipocyte-driven model prompted by the findings of Nieman *et al.*, showed that in omental metastases, ovarian cancer cells at the interface with adipocytes contained abundant lipids (41). *In vitro* studies showed that the adipocytes transfer lipid droplets that contain fatty acids to ovarian cancer cells (41), that can be used as an energy source The strength of their studies is that they focused on human ovarian cancers and identified a novel function for adipocytes in the progressive growth of ovarian cancer lesions. The weakness of this work lies in its effort to show that adipocytes drive, and are solely responsible for, early steps in omental colonization. The case for adipose as the sole determinant of the ovarian cancer's organotropic metastasis was based on an incomplete examination of the literature and a biased approach to experimental design. As a result of the focus on adipocytes, important clues in the data were overlooked and the potential contributions of milky spots, vasculature, or other unique characteristics of the omentum were neither tested nor discussed. Thus, like the milky spot-driven model, this model is also limited by the narrow focus of the studies upon which it was based.

Despite their strengths, neither the milky spot-driven nor the adipocyte-driven models address the intimate and dynamic interactions among milky spot structures, adipocytes, and other omental components. Integration of these two models required a fresh look from a different perspective. Thus, we sought to understand why ovarian cancers *do not colonize* other sources of peritoneal fat as extensively as they do the omentum, rather than more traditional omentum-focused approaches. This led to our novel strategy to compare colonization of peritoneal adipose that either contains or lacks milky spots. The report by Takemori *et al* (42), showing the presence of milky spots in the splenoportal fat of New Zealand Black mice was key to our approach. To our knowledge, the splenoportal fat band has not been studied in other mouse strains, nor has its colonization by any type of cancer cells been examined prior to the work presented herein. *In vivo* studies using a panel of ovarian cancer cell lines (ID8, SKOV3ip.1, CaOV3, and HeyA8) yielded the most comprehensive assessment of ovarian cancer cell lodging in peritoneal adipose and provided clear data showing that milky spots dramatically enhance early cancer cell lodging.

To dissect the mechanism(s) by which milky spots promote colonization, we made use of the observation that after i.p. injection, ovarian cancer cells rapidly localize to omental milky spots, suggesting involvement of a tissue-secreted factor(s). Development of the quantitative transwell migration approach (Figure 4) enabled us to assess the ability of fat (tissue)-conditioned media to stimulate directed migration of ovarian cancer cells. Although milky spot-deficient tissues (uterine fat, gonadal fat and mesentery) secrete one or more factors that promotes directed migration, results from *in vivo* assays indicate that this signal is not sufficient for ovarian cancer cells to achieve the high level (both number and size) of foci formation seen in the omentum and splenoportal fat. This suggests that colonization requires additional chemotactic signals and/or tissue structures. In support of this notion, *in vivo* assays showed that ovarian cancer cells efficiently colonize milky spots in the omentum and splenoportal fat. In addition, using media conditioned by milky spot-containing adipose yielded the novel finding that the presence of these structures caused a significant enhancement in the media's ability to promote directed cancer migration.

Our findings show the critical importance of milky spots to ovarian cancer cell lodging and initial colonization of peritoneal adipose (3, 6, 21, 25, 36-40) and provide a foundation for studies to identify milky spot components involved in cancer cell homing and invasion. As a first step toward this goal, the use of immunodeficient mouse strains allowed us to rule out a requirement for B cells, T cells, or NK cells for ovarian cancer cell lodging within milky spots, confirming and expanding on the findings

of Lotan *et al.* (8) Previous studies have shown that mast cells and macrophages are frequently observed in the milky spots (27, 30, 31, 33). Macrophages are an intriguing candidate as they have been shown to assist the survival and growth of established tumors (43-45). Further, the depletion of peritoneal macrophages has been shown to decrease ovarian cancer tumor burden on the diaphragm at the experimental endpoint (46). Milky spot macrophages are thus possibly contributing to the rapid and specific colonization of omental milky spots. Another possible source of the omentum's chemotactic properties is the abundance of endothelial cells found in the milky spots. The vessels within the dense and tangled capillary bed of the milky spots have been shown to undergo a constitutive level of active vascular remodeling (25, 38). The activated endothelial cells associated with angiogenic vessels are known to support and promote metastatic disease (47, 48). Either or both of those cell types could be responsible for the prolific omental metastases and warrant future study.

The growing emphasis on the role of the host tissue microenvironment in metastasis formation stems from the seminal work of Stephen Paget showing that certain tumor cells (the "seed") have a proclivity for specific organ microenvironment(s) (the "soil") (49-51). A powerful but often underappreciated aspect of studies by Paget and other pioneers of metastasis research was their innate appreciation of the unique tissue architecture, physiology, and function of the target organ that is essential to understanding metastatic organ specificity (51-55). The studies presented herein seek to integrate milky spot and adipocyte function in the omentum. We propose a two-step model for omental colonization wherein the localization of disseminated cancer cells is dependent upon milky spots. Adipocytes are then required for progressive growth and subsequent spread of cancer cells to other sites within the peritoneal cavity. This model is likely a more accurate representation of the overall process of ovarian metastatic colonization. It is our hope that both our findings and discussion of the larger literature will serve as a framework for studies that will continue to refine our understanding of omental colonization. Ultimately, it is our goal to use this information to extend the duration of metastatic suppression and significantly increase the quality of life for patients diagnosed with ovarian cancer.

References:

1. Naora H, Montell DJ: Ovarian Cancer Metastasis: Integrating insights from disparate model organisms. Nat Rev Cancer 2005, 5:355–366.
2. Cinti S: The Adipose Organ. In: Fantuzzi G, mazzone T, editors. Adipose Tissue and Adipokines in Health and Disease, Totowa, New Jersey, Humana Press, 2007, pp. 3–19.
3. Hagiwara A, Takahashi T, Sawai K, Taniguchi H, Shimotsuma M, Okano S, Sakakura C, Tsujimoto H, Osaki K, Sasaki S: Milky spots as the implantation site for malignant cells in peritoneal dissemination in mice. Cancer Research, AACR, 1993, 53:687.
4. Roby KF, Taylor CC, Sweetwood JP, Cheng Y, Pace JL, Tawfik O, Persons DL, Smith PG, Terranova PF: Development of a syngeneic mouse model for events related to ovarian cancer. Carcinogenesis 2000, 21:585–591.
5. Lengyel E: Ovarian Cancer Development and Metastasis. The American Journal of Pathology, American Society for Investigative Pathology, 2010, 177:1053–1064.
6. Khan SM, Funk HM, Thiolloy S, Lotan TL, Hickson J, Prins GS, Drew AF, Rinker-Schaeffer CW: In vitro metastatic colonization of human ovarian cancer cells to the omentum. Clin Exp Metastasis 2010, 27:185–196.
7. Kenny HA, Krausz T, Yamada SD, Lengyel E: Use of a novel 3D culture model to elucidate the role of mesothelial cells, fibroblasts and extra-cellular matrices on adhesion and invasion of ovarian cancer cells to the omentum. Int J Cancer 2007, 121:1463–1472.
8. Liebermann-Meffert D: The greater omentum. Anatomy, embryology, and surgical applications. Surg Clin North Am 2000, 80:275–93–xii.
9. Collins D, Hogan AM, O'Shea D, Winter DC: The omentum: anatomical, metabolic, and surgical aspects. J Gastrointest Surg 2009, 13:1138–1146.
10. Platell C, Cooper D, Papadimitriou JM, Hall JC: The omentum. World J Gastroenterol 2000, 6:169–176.
11. Goldsmith HS: The Omentum: Basic Research and Clinical Application. 1st ed. Goldsmith HS, editor. New York, Cine Med, Inc, 1990.
12. Wilkosz S, Ireland G, Khwaja N, Walker M, Butt R, Giorgio-Miller A, Herrick SE: A comparative study of the structure of human and murine greater omentum. Anat Embryol 2005, 209:251–261.
13. Wozniak SE, Gee LL, Wachtel MS, Frezza EE: Adipose Tissue: The New Endocrine Organ? A Review Article. Dig Dis Sci 2008, 54:1847–1856.
14. Trayhurn P, Beattie JH: Physiological role of adipose tissue: white adipose tissue as an endocrine and secretory organ. Proc Nutr Soc 2001, 60:329–339.
15. Hauner H: The new concept of adipose tissue function. Physiol Behav 2004, 83:653–658.
16. Scherer PE: Adipose tissue: from lipid storage compartment to endocrine organ. Diabetes 2006, 55:1537–1545.
17. Kershaw EE, Flier JS: Adipose tissue as an endocrine organ. J Clin Endocrinol Metab 2004, 89:2548–2556.
18. Wang P, Mariman E, Renes J, Keijer J: The secretory function of adipocytes in the physiology of white adipose tissue. J Cell Physiol 2008, 216:3–13.
19. Conde J, Scotece M, Gómez R, López V, Gómez-Reino JJ, Lago F, Gualillo O: Adipokines: biofactors from white adipose tissue. A complex hub among inflammation, metabolism, and immunity. Biofactors 2011, 37:413–420.
20. Rajala MW, Scherer PE: Minireview: The adipocyte--at the crossroads of energy homeostasis,

inflammation, and atherosclerosis. Endocrinology 2003, 144:3765–3773.

21. Michailova KN, Usunoff KG: The milky spots of the peritoneum and pleura: structure, development and pathology. Biomedical Reviews, Varna, Bulgaria, 2004, 15:47–66.

22. Simer P: On the morphology of the omentum, with especial reference to its lymphatics. American Journal of Anatomy, Wiley Subscription Services, Inc., A Wiley Company, 1934, 54:203–228.

23. Ackermann PC, De Wet PD, Loots GP: Microcirculation of the rat omentum studied by means of corrosion casts. Acta Anat (Basel) 1991, 140:146–149.

24. Shimotsuma M, Shields J, Simpson-Morgan M, Sakuyama A, Shirasu M, Hagiwara A, Takahashi T: Morpho-physiological function and role of omental milky spots as omentum-associated lymphoid tissue (OALT) in the peritoneal cavity. Lymphology 1993, 26:90.

25. Gerber SA, Rybalko VY, Bigelow CE, Lugade AA, Foster TH, Frelinger JG, Lord EM: Preferential Attachment of Peritoneal Tumor Metastases to Omental Immune Aggregates and Possible Role of a Unique Vascular Microenvironment in Metastatic Survival and Growth. The American Journal of Pathology, American Society for Investigative Pathology, 2006, 169:1739–1752.

26. Shimotsuma M, Kawata M, Hagiwara A, Takahashi T: Milky spots in the human greater omentum. Macroscopic and histological identification. Acta Anat (Basel) 1989, 136:211–216.

27. Shimotsuma M, Simpson-Morgan MW, Takahashi T, Hagiwara A: Activation of omental milky spots and milky spot macrophages by intraperitoneal administration of a streptococcal preparation, OK-432. Cancer Research 1992, 52:5400–5402.

28. Litbarg NO, Gudehithlu KP, Sethupathi P, Arruda JAL, Dunea G, Singh AK: Activated omentum becomes rich in factors that promote healing and tissue regeneration. Cell Tissue Res 2007, 328:487–497.

29. Rangel-Moreno J, Moyron-Quiroz JE, Carragher DM, Kusser K, Hartson L, Moquin A, Randall TD: Omental Milky Spots Develop in the Absence of Lymphoid Tissue-Inducer Cells and Support B and T Cell Responses to Peritoneal Antigens. Immunity, Elsevier Ltd, 2009, 30:731–743.

30. Wijffels JF, Hendrickx RJ, Steenbergen JJ, Eestermans IL, Beelen RH: Milky spots in the mouse omentum may play an important role in the origin of peritoneal macrophages. Res Immunol 1992, 143:401–409.

31. Shimotsuma M, Takahashi T, Kawata M, Dux K: Cellular subsets of the milky spots in the human greater omentum. Cell Tissue Res 1991, 264:599–601.

32. Cranshaw ML, Leak LV: Milky spots of the omentum: a source of peritoneal cells in the normal and stimulated animal. Arch Histol Cytol 1990, 53 Suppl:165–177.

33. Beelen RH, Fluitsma DM, Hoefsmit EC: The cellular composition of omentum milky spots and the ultrastructure of milky spot macrophages and reticulum cells. J Reticuloendothel Soc 1980, 28:585–599.

34. Krist LF, Eestermans IL, Steenbergen JJ, Hoefsmit EC, Cuesta MA, Meyer S, Beelen RH: Cellular composition of milky spots in the human greater omentum: an immunochemical and ultrastructural study. Anat Rec 1995, 241:163–174.

35. Mironov VA, Gusev SA, Baradi AF: Mesothelial stomata overlying omental milky spots: scanning electron microscopic study. Cell Tissue Res 1979, 201:327–330.

36. Krist LF, Kerremans M, Broekhuis-Fluitsma DM, Eestermans IL, Meyer S, Beelen RH: Milky spots in the greater omentum are predominant sites of local tumour cell proliferation and accumulation in the peritoneal cavity. Cancer Immunol Immunother 1998, 47:205–212.

37. Green JA, Williams AE: The relationship between inflammatory responses and WBP1 tumour cell attachment to the rat omentum. Eur J Cancer 1978, 14:1153–1155.

38. Sorensen EW, Gerber SA, Sedlacek AL, Rybalko VY, Chan WM, Lord EM: Omental immune aggregates and tumor metastasis within the peritoneal cavity. Immunol Res 2009, 45:185–194.

39. Tsujimoto H, Takhashi T, Hagiwara A, Shimotsuma M, Sakakura C, Osaki K, Sasaki S, Shirasu M, Sakakibara T, Ohyama T: Site-specific implantation in the milky spots of malignant cells in peritoneal dissemination: immunohistochemical observation in mice inoculated intraperitoneally with bromodeoxyuridine-labelled cells. Br J Cancer, Nature Publishing Group, 1995, 71:468.

40. Tsujimoto H, Hagiwara A, Shimotsuma M, Sakakura C, Osaki K, Sasaki S, Ohyama T, Ohgaki M, Imanishi T, Yamazaki J, Takahashi T: Role of milky spots as selective implantation sites for malignant cells in peritoneal dissemination in mice. J Cancer Res Clin Oncol 1996, 122:590–595.

41. Nieman KM, Kenny HA, Penicka CV, Ladanyi A, Buell-Gutbrod R, Zillhardt MR, Romero IL, Carey MS, Mills GB, Hotamisligil GS, Yamada SD, Peter ME, Gwin K, Lengyel E: Adipocytes promote ovarian cancer metastasis and provide energy for rapid tumor growth. Nat Med 2011, 17:1498–1503.

42. Takemori N, Hirai K, Onodera R, Saito N, Namiki M: Light and electron microscope study of splenoportal milky spots in New Zealand black mice: comparison between splenoportal milky spots and aberrant spleens. J Anat 1995, 186 (Pt 2):287–299.

43. Qian B-Z, Pollard JW: Macrophage diversity enhances tumor progression and metastasis. Cell 2010, 141:39–51.

44. Tlsty TD, Coussens LM: Tumor stroma and regulation of cancer development. Annu Rev Pathol 2006, 1:119–150.

45. Coussens LM, Werb Z: Inflammation and cancer. Nature 2002, 420:860–867.

46. Robinson-Smith TM, Isaacsohn I, Mercer CA, Zhou M, Van Rooijen N, Husseinzadeh N, McFarland-Mancini MM, Drew AF: Macrophages Mediate Inflammation-Enhanced Metastasis of Ovarian Tumors in Mice. Cancer Research 2007, 67:5708–5716.

47. Orr FW, Wang HH, Lafrenie RM, Scherbarth S, Nance DM: Interactions between cancer cells and the endothelium in metastasis. J Pathol, Wiley Online Library, 2000, 190:310–329.

48. Chouaib S, Kieda C, Benlalam H, Noman MZ, Mami-Chouaib F, Rüegg C: Endothelial cells as key determinants of the tumor microenvironment: interaction with tumor cells, extracellular matrix and immune killer cells. Crit Rev Immunol 2010, 30:529–545.

49. Paget S: The distribution of secondary growths in cancer of the breast. 1889. The Lancet 1889, 133:571–573.

50. Kenny PA, Bissell MJ: Tumor reversion: correction of malignant behavior by microenvironmental cues. Int J Cancer 2003, 107:688–695.

51. Bissell MJ, Radisky DC, Rizki A, Weaver VM, Petersen OW: The organizing principle: microenvironmental influences in the normal and malignant breast. Differentiation 2002, 70:537–546.

52. Nicolson GL: Organ specificity of tumor metastasis: role of preferential adhesion, invasion and growth of malignant cells at specific secondary sites. Cancer Metastasis Rev 1988, 7:143–188.

53. Fidler IJ: The pathogenesis of cancer metastasis: the “seed and soil” hypothesis revisited. Nat. Rev. Cancer. 2003, pp. 453–458.

54. Hart IR, Fidler IJ: Role of Organ Selectivity in the Determination of Metastatic Patterns of B16 Melanoma. Cancer Research 1980.

55. Sugarbaker EV: Cancer metastasis: a product of tumor-host interactions. Curr Probl Cancer 1979, 3:1–59.

Appendices: Manuscript Submitted

THE UNIVERSITY OF CHICAGO
BIOLOGICAL SCIENCES

Chicago, IL 60637-1470

DEPARTMENT OF SURGERY
Section of Urology
5841 South Maryland Avenue

Phone: (773) 702-5882
Lab: (773) 702-3140
Fax: (773) 702-1001

Carrie W. Rinker-Schaeffer, Ph.D.
Full Professor
Director of Urology Research

September 24, 2012

Michael P. Lisanti, M.D., Ph.D.,
Editor in Chief, *The American Journal of Pathology*,
9650 Rockville Pike, Bethesda,
Maryland, USA 20814-3993.

Dear Dr. Lisanti

Enclosed please find our manuscript, "Milky spots are required for ovarian cancer colonization of peritoneal adipose depots" submitted by Clark and Krishnan *et al*., for consideration for publication in **The American Journal of Pathology**, as a **Research Article**. We believe that this work is ideally suited for your Journal as it focuses on the role of omental tissue composition and architecture in the pathological process of ovarian cancer metastatic colonization. It also presents a scholarly appraisal of omental tissue physiology and function and its potential contributions to ovarian cancer metastasis, which sadly has been overlooked by the ovarian cancer community. Consistent with the Journal's mission, this work will advance our basic and translational knowledge of ovarian cancer metastasis formation. The work uses physiologically relevant experimental models, and a combination of cellular, molecular, animal, and immunological approaches in conjunction with tissue morphology.

Work in this manuscript seeks to understand the role of the tissue microenvironment(s) in ovarian cancer cell lodging and progressive growth within the omentum, a preferred site of ovarian cancer metastasis formation. The omentum's tissue architecture is unusual in that its adipocyte-rich regions contain milky spots, structures consisting of immune cells, stromal cells and structural elements surrounding glomerulus-like capillary beds. Contrary to previous reductionist studies, our findings show that both milky spots and adipocytes play distinct, complementary roles in metastasis.

Specifically, metastasis assays using ID8 and SKOV3ip.1 ovarian cancer cells, showed that cells only lodge and grow within omental and splenoportal fat, which contain milky spots, and not other peritoneal fat depots. Similarly, media conditioned by milky spot-containing adipose tissue caused 72% more cell migration than media conditioned by milky spot-deficient adipose. Studies using a panel of immune-deficient mice showed that the

mouse genetic background does not alter omental milky spot number and size, nor does it effect ovarian cancer colonization. Finally, consistent with the role for lipids as an energy source for cancer cell growth, *in vivo* time-course studies found an inverse relationship between metastatic burden and omental adipocyte content. Our findings support a two-step model wherein both milky spots and adipose have specific roles in colonization of the omentum by ovarian cancer cells.

On behalf of the authors I can affirm that we have no financial conflict of interests to declare. I can also affirm that the manuscript has not been published previously and is not being considered concurrently by another publication, and affirm that all authors and acknowledged contributors have read and approved the manuscript. We cite a scientific conflict with Dr. Ernst Lengyel M.D., Department of Obstetrics and Gynecology, The University of Chicago. To facilitate the review process we have suggested members of the Editorial Board and larger scientific community that we believe are appropriate for the review of this manuscript. Please feel free to contact me if I can be of further assistance in this review process. Thank you in advance for your efforts on our behalf.

Most Sincerely,

Carrie Rinker-Schaeffer, Ph.D.
President of the Metastasis Research Society
Departments of Surgery and Obstetrics and Gynecology
Committee of Cancer Biology
Committee on Genetics, Genomics and Systems Biology

Dr. Deborah Armstrong, Director Breast and Ovarian Surveillance Service
Johns Hopkins Sidney Kimmel Comprehensive Cancer Center
The Bunting-Blaustein Cancer Research Building-1
1650 Orleans Street, Room 190
Baltimore, Maryland 21231-1000
Tel: 410.614.2743 **Fax:** 410.955.0125 **Email:** armsrde@jhmi.edu

Dr. Ann Chambers, Distinguished Oncology Scientist
London Regional Cancer Program
Room A4-903b
790 Commissioners Rd. E.
London, Ontario
Canada N6A 4L6
Tel: **Fax:** **Email:** Ann.Chambers@lhsc.on.ca

Dr. Victoria Seewaldt, Professor
Leader Breast and Ovarian Cancer Program
Duke University Comprehensive Cancer Center
Department of Medicine
Rm 221A MSRB
DUMC 2628
Durham, NC 27710
Tel: **Fax:** **Email:** seewa001@mc.duke.edu

Dr. Patricia Steeg, Chief, Women's Cancers Section
Laboratory of Molecular Pharmacology
Center for Cancer Research, National Cancer Institute
Building 37, Room 1122
Bethesda, MD 20892
Tel: **Fax:** **Email:** steegp@mail.nih.gov

Dr. Ann Thor, Professor and Chair, Department of Pathology
University of Colorado Denver, School of Medicine
Department of Pathology
12631 E 17th Avenue, Room L15-2215
Mail Stop B216
Aurora, CO 80045
Tel: **Fax:** **Email:** Ann.Thor@ucdenver.edu

Milky spots are required for ovarian cancer colonization of peritoneal adipose depots

Robert Clark[1,&], Venkatesh Krishnan[2,&], Michael Schoof[2,§], Irving Rodriguez[2,§], Betty Theriault[3], Marina Chekmareva[4] and Carrie Rinker-Schaeffer[2,#]

[1]Department of Molecular Pathogenesis and Molecular Medicine, The University of Chicago, Chicago, IL

[2]The Section of Urology, Department of Surgery, The University of Chicago, Chicago, IL

[3]Department of Surgery and the Animal Resources Center, The University of Chicago, Chicago, IL

[4]Department of Pathology, Robert Wood Johnson Medical School, New Brunswick, NJ

[&]Authors contributed equally to this work

[§]Current address: Department of Natural Sciences, Stanford University, Stanford, CA

[#] To whom correspondence should be addressed:
Section of Urology, Department of Surgery, MC6038
The University of Chicago
5841 South Maryland Avenue
Chicago, IL 60637
Tel: 773-702-5882
Fax: 773-702-1001
Email: crinkers@uchicago.edu

Number of Text Pages: 42

Number of Tables: 0

Number of Figures: 7 Primary; 4 Supplemental

Short Running Title: Ovarian cancer colonizes milky spots

Financial Support
Work was supported by grants from the DOD (W81XWH-09-1-0127), NCI/NIH (2RO1CA089569), and Elsa U. Pardee Foundation; Marsha Rivkin Center for Ovarian Cancer Research Pilot Study Award; and funds from the Section of Urology (The University of Chicago)

Keywords: ovarian cancer, omentum, milky spots, peritoneal fat, splenoportal fat

Abstract

Control of ovarian cancer metastasis formation requires identification and understanding of the specific tissue microenvironments involved in cancer cell colonization of the omentum. Omental adipose is a site of prodigious metastasis in both ovarian cancer models and clinical disease. It is unusual as its adipocyte-rich regions contain milky spots, structures consisting of immune cells, stromal cells and structural elements surrounding glomerulus-like capillary beds. Contrary to previous reductionist studies, work presented herein shows that milky spots and adipocytes play distinct, complementary roles in metastasis. Specifically, metastasis assays using ID8 and SKOV3ip.1 ovarian cancer cells showed that cells only lodge and grow within omental and splenoportal fat, which contain milky spots, and not other peritoneal fat depots. Similarly, media conditioned by milky spot-containing adipose tissue caused 75% more cell migration than media conditioned by milky spot-deficient adipose. Studies using a panel of immunodeficient mice showed that the mouse genetic background does not alter omental milky spot number and size, nor does it affect ovarian cancer colonization. Finally, consistent with the role for lipids as an energy source for cancer cell growth, *in vivo* time-course studies found an inverse relationship between metastatic burden and omental adipocyte content. Our findings support a two-step model wherein both milky spots and adipose have specific roles in colonization of the omentum by ovarian cancer cells.

Introduction

It is estimated that in 2012 nearly 23,000 American women will be diagnosed with ovarian cancer and 16,000 will die of their disease.[1] The majority of patients present with metastasis or eventually succumb to metastatic disease within the abdominal cavity.[1] After escape from the primary tumor, ovarian cancer cells populate the peritoneal fluid and have access to and can potentially lodge within a variety of tissues.[2,3] However, in both clinical disease and experimental models, the omentum is a site of prodigious metastasis formation.[4-7] Thus, attachment of ovarian cancer cells to the omentum represents a rate-limiting step in metastasis formation.[8,9] Although the importance of the omentum is widely acknowledged, there still is no consensus on the role its microenvironment plays in ovarian cancer metastasis formation. This raises the question, "How do ovarian cancer cells specifically colonize the omental tissue microenvironment?"

Studies of omental function date back to Jobert de Lamballe, a military surgeon to Napoleon I, who was reportedly the first to recognize its curious ability to fight injection and form adhesions to help control injuries.[10] As a result of nearly two centuries of investigation, a great deal is known about the omentum's physiology and surgical applications.[10-13] As the central regulator of peritoneal homeostasis, its functions include: regulating fluid and solute transport, sensing and repairing injuries, promoting angiogenesis, fighting infection, serving as a source of stem cells, production of regulatory molecules and storing and supplying lipids. Remarkably, these diverse functions are conferred by the interaction of the two structurally distinct tissue types that compose it. The *translucent membranes* are composed of collagen fibers and fibroblast-like cells enclosed by two closely opposed mesothelial cell layers that assemble into a net-like structure with large fenestrations throughout.[14,15] The fenestrations

are thought to be involved in both fluid transport and adhesion formation. A role for this tissue in metastatic colonization has not been reported.

In contrast, the *adipose-rich areas* are composed of adipocytes, immune cells, stromal cells and connective matrix components that lay beneath an irregular mesothelium. Adipocytes have a variety of functions, ranging from lipid storage to production of endocrine molecules.[3,16-21] The adipose can also serve as an integrating hub for inflammation, metabolism and immunity.[22-25] A distinctive feature of the vasculature in omental adipose is the presence of numerous branching blood vessels ending in tortuous glomerulus-like capillary beds near the tissue periphery.[26-30] Immune cells aggregate around and within these glomeruli to form milky spots: the major immune structure for host defense of the peritoneal cavity.[26,31-38] In most milky spots, both the endothelial lining of the omental capillaries and the overlying mesothelium are specially adapted to facilitate transmigration of immune cells.[26,39,40] Additional structural elements include plasmocytes, fibroblasts and mesenchymal cells, as well as collagen, reticular and elastic fibers.[31,36,39,41]

A comprehensive literature review showed that studies examining omental metastasis take a reductionist approach and focus on the role of individual components of the adipose-rich region. In our view, results from the majority of studies support models in which ovarian cancer metastatic colonization is either purely "milky spot-driven" or purely "adipocyte-driven." The milky spot-driven model is based on a large body of *in vivo* data showing that after i.p. injection, cancer cells rapidly and specifically localize to, invade and proliferate within omental milky spots.[4,7,26,30,42-46] An implication of this model is that cells within milky spots produce chemotactic factors potentially responsible for cancer cell homing to and invasion of milky spots, as well as provide a conducive microenvironment for cancer cell survival and growth.[30,34,42] In contrast, the adipocyte-driven model is based on the observation that in its

resting state, the omentum is predominantly composed of adipose. Furthermore, cultured adipocytes can produce adipokines capable of promoting ovarian cancer cell migration and invasion *in vitro*.[47] Additional studies showed that adipocytes could also provide a proliferative advantage by transferring fatty acids to ovarian cancer cells.[47] Although there are clear strengths to both of these models, neither addresses the intimate and dynamic interaction between milky spot structures, adipocytes and other components of the adipose-rich region.

Using tissue architecture and function as a guide, we propose that an alternative, more fully integrated model of metastatic colonization is needed. To test this we identified peritoneal fat deposits (omentum, mesentery, uterine, gonadal and splenoportal fat) that are accessible to ovarian cancer cells after i.p. injection.[3] Of these, the omentum and splenoportal fat are reported to contain analogous milky spots.[48] We reasoned that a comparison of peritoneal adipose that either contain or lack milky spots could be used to determine the contributions of adipocytes and milky spots to the lodging and progressive growth of ovarian cancer cells in physiologically relevant tissues. *In vivo* studies showed that milky spots are an absolute requirement for cancer cell lodging on peritoneal adipose. Consistent with this finding, conditioned media from milky spot-containing adipose tissue has an enhanced ability to direct cell migration as compared to conditioned media from milky spot-deficient adipose tissue. Studies using a panel of immune-deficient mice showed that the number and size of omental milky spots is not dependent on the mouse genetic background. Similarly, ovarian cancer cell colonization does not depend on the immune composition of the milky spot. Finally, consistent with the role for lipids as an energy source for ovarian cancer cell growth, *in vivo* time-course studies found an inverse relationship between metastatic burden and adipocyte content in the omentum. Our findings support a

two-step model wherein both milky spots and adipose have specific roles in colonization of the omentum by ovarian cancer cells.

Materials and Methods

Cell Lines: The SKOV3ip.1 human ovarian carcinoma cell line[49] was a generously supplied by Dr. Gordon Mills (M.D. Anderson Cancer Center, Houston, TX). These cells were maintained in standard growth media [DMEM containing D-glucose (4.5 g/L), L-glutamine (584 mg/L) and sodium pyruvate (110 mg/L) (Mediatech, Manassas, VA), supplemented with 5% Fetal Bovine Serum (FBS; Atlanta Biologicals, Lawrenceville, GA), 1% Penicillin/Streptomycin (P/S) solution (5,000 IU/ml Penicillin + 5,000 µg/ml Streptomycin mixture), 1X non-essential amino acids and 2X MEM vitamin solution (all from Mediatech)]. The ID8 mouse ovarian carcinoma cell line, derived from and syngeneic to mice of the C57Bl/6 background[5], was generously provided by Dr. Katherine Roby (University of Kansas Medical Center, Kansas City, KS). These cells were maintained in a standard growth media [DMEM supplemented with 4% FBS, 1% P/S solution and 5 µg/ml insulin-transferrin-sodium selenite (Roche, Indianapolis, IN)]. All cells were maintained under standard tissue culture conditions (i.e. in a humidified incubator at 37°C supplemented with 5% CO_2).

Mice: All mice were housed and maintained according to Institutional Animal Care and Use guidelines and under the supervision of the University of Chicago Animal Resource Center. Outbred CD1 mice were obtained from Charles River (Wilmington, MA). Inbred B6 (C57Bl/6NHsd; immunocompetent), Nude (Athymic Nude-*Foxn1*^{nu}; which are T cell deficient) and BN XID (Hsd:NIHS-*Lyst*^{bg}*Foxn1*^{nu}*Btk*^{xid}; which are NK cell and T cell deficient) mice were obtained from Harlan Laboratories (Indianapolis, IN). Rag1 (B6.129S7-*Rag1*^{tm1Mom}*/J*; which have no mature T or B cells, no CD3 positive and no T cell receptor α-β positive cells) and

157 Igh6 (B6.129S2-*Ighm*^{tm1Cgn}/*J*; which lack mature B cells) mice were obtained from Jackson
158 Laboratories (Bar Harbor, ME).

159 **Harvesting Mouse Tissues:** The locations of the well-defined depots of adipose used for the
160 studies described herein are described.[3] Omenta were harvested as described by Khan *et*
161 *al.*[7] Splenoportal fat bands were collected by isolating the thin, fatty band of tissue connecting
162 the hilum of the spleen to the pancreas,[48] releasing it from the pancreas and then carefully
163 dissecting it from the spleen. Uterine fat was excised from the uterine horns using dissecting
164 scissors. Similarly, gonadal fat was excised from the ovaries. Mesenteries were collected by
165 first cutting the junction between the small intestine and the pylorus, firmly gripping the free
166 end of the small intestine with forceps, "peeling" the small intestine from the mesentery by
167 pulling the tissue slowly and finally releasing the mesentery from the mesentery root with
168 dissecting scissors.

169 **Preparation of Tissues for Standard Histologic Evaluation:** Tissues were processed for
170 histological evaluation immediately after harvest or *ex vivo* culture. Larger tissues (whole
171 gonadal fat, uterine fat and mesentery) were fixed in 10% neutral buffered formalin (Sigma
172 Aldrich, St. Louis, MO) for 48 hrs at 4°C. Smaller tissues (whole omentum, splenoportal fat
173 and tissue equivalents of uterine fat and mesentery) were fixed overnight (12-16 hrs) in 5%
174 neutral buffered formalin (Sigma Aldrich) at 4°C. Fixed tissue was stored in 70% ethanol at
175 4°C until it was embedded in paraffin. Tissues were sectioned (4 μm) and hematoxylin &
176 eosin (H&E) stained by the University of Chicago Human Tissue Resource Center. All
177 pathological evaluation of tissue was performed by MC under blind conditions.

178 **Immunohistochemistry:** Tissue sections were deparaffinized in xylenes and rehydrated
179 through serial dilutions of ethanol to distilled water. Sections were subsequently incubated in
180 antigen retrieval buffer (DAKO, Carpinteria, CA) and heated in steamer to 97°C for 20 min.

Primary antibodies were diluted in Tris Buffered Saline and Tween (TBST) with 0.025% Triton X-100. Pan-cytokeratin (clone: H-240 #sc-15367, Santa Cruz Biotechnology, Santa Cruz, CA) and CD45 (clone: H130 #14-0459-82, eBioscience, San Diego, CA) were applied to tissue sections at a 1:100 dilution and incubated for 1 hr at room temperature. After application of primary antibody, slides were rinsed in Tris-Buffered Saline (TBS) and biotinylated secondary antibody, diluted in TBST with 10% mouse serum (Jackson ImmunoResearch, West Grove, PA) was applied to the slides. For pan-cytokeratin staining, sections were incubated with goat anti-rabbit IgG (1:200 dilution, #BA-1000, Vector Laboratories, Burlingame, CA) for 30 min at room temperature. For CD45 staining, sections were incubated with anti-mouse IgG (1:100 dilution, #BA-2001, Vector Laboratories) for 30 min at room temperature. The biotinylated secondary antibody was detected using the Vectastain Elite ABC kit (Vector Laboratories) and DAB (DAKO) peroxidase substrate.

Peritoneal Metastasis Assay: Exponentially growing SKOV3ip.1 or ID8 cells were trypsinized and prepared as a single cell suspension at a concentration of $2x10^6$ cells/ml in cold phosphate buffered saline (PBS). Animals were injected intraperitoneally with 500 µl of the cell suspension (1×10^6 cells) at a point equidistant between the inguinal papilla. For all experiments, 500 µl of cold PBS was injected as a negative control in a parallel group of control mice. At the experimental endpoint of each assay, mice were sacrificed via CO_2 asphyxiation. Tissues were then harvested, processed, sectioned and stained as described herein.

Preparation of Tissue-Conditioned Media: Tissues were harvested under sterile conditions and immediately placed in sterile cold PBS. After collection, “tissue equivalents” were prepared by first weighing the omentum from an individual mouse and then excising a strip of uterine fat or branch of mesentery of equivalent weight. In our studies we found that a single

band of splenoportal fat weighs 2.90 ± 0.62 mg (mean ± 2SD). Given that this is approximately one half the weight of an omentum (6.72 ± 2.82 mg), two fat bands were combined to make one tissue equivalent. Each tissue equivalent was placed in its own well of a polystyrene 12-well plate containing 1.25 ml DMEM/F-12 supplemented with 20% FBS and 1% P/S and incubated at 37°C with 5% CO_2 as described by Khan *et al.*[7] Tissues were allowed to acclimate to these *ex vivo* conditions for 24 hrs after which the serum-containing media was removed, tissues were carefully rinsed with PBS and then placed in 1.25 ml serum-free DMEM/F-12 (containing 1% P/S). After 24 hrs of conditioning, the serum-free media was collected and used for the transwell migration assays as described. For longer *ex vivo* culture, media was changed to fresh serum-free DMEM/F12 at subsequent 24 hr intervals, such that the tissues were fed for the first 24hrs and starved for the remainder of the assay. Conditioned media from each 24hr interval was collected. In order to ensure that stimulatory activity in the conditioned media was due to secretion of chemotactic factors and not cellular breakdown, tissue integrity was assessed by H&E staining and light microscopy as described by Khan *et al.*[7] Tissue integrity was further assessed by manually counting the number of healthy and necrotic adipocytes on H&E sections and formulating a percentage of live tissue present. Tissue function was also confirmed by measuring interleukin-6 (IL-6) levels in the conditioned media. IL-6 is produced by adipose, mesothelial cells and immune cells and immediately secreted into the microenvironment.[50] Specifically, enzyme-linked immunosorbent assays (ELISA) for IL-6 were performed on tissue-conditioned media using a Mouse IL-6 Platinum ELISA kit (eBioscience, San Diego, CA) following the manufacturers instructions.

Transwell Migration Assay: All migration assays used the same physical setup with 1 mL of conditioned or control media (unconditioned culture media) to be tested for chemoattractant

activity placed in the lower chamber and cancer cells placed in 8 µm-pore PET membrane transwell (BD Falcon, Franklin Lakes, NJ) which served as the upper chamber of the assay apparatus. Exponentially growing SKOV3ip.1 or ID8 cells were trypsinized and resuspended in serum-free DMEM at a concentration of 3.33 x 10^5 cells/ml or 2.50 x 10^5 cells/ml, respectively. In each case, 600 µl of cell suspensions (SKOV3ip.1 = 2.0 x 10^5 total; ID8 = 1.5 x 10^5 total) were added to the transwells. Cells were allowed to migrate in response to signals from conditioned or control media for 6 hrs under standard tissue culture conditions.

After incubation, media was aspirated from both chambers and the upper and lower surfaces of the membrane were washed once with cold PBS. The membrane was fixed in 10% buffered formalin for 10 min at room temperature. Residual formalin was removed by washing with cold PBS. Both sides of the membrane were subsequently stained with a 0.05% crystal violet solution (Fisher, Fair Lawn, NJ) for 30 min at room temperature and washed once with tap water. Cells that had not migrated through the membrane were removed by gently wiping the upper membrane surface with a cotton swab and the membrane was allowed to air-dry overnight. Finally, the membrane was removed from the transwell scaffold using a scalpel and mounted top-surface-facing-up onto a slide using Permount as the mounting medium (Fisher). The number of cells that had migrated through the membrane was quantified by taking 5 random images per slide at 100x with an Axiovert 200M inverted microscope (University of Chicago Integrated Microscopy Core Facility). ImageJ (NIH) was used to quantitate the total number of migrated cells present in each image. The counts from each of the five images were totaled to give the number of migrated cells for each sample. n= 5 for all conditions.

Milky Spot Identification Using Carbon Nanopowder Uptake: Carbon nanopowder was used to stain milky spot phagocytes similarly to described methods.[31] Briefly, carbon (<50 nm

particle size; Sigma Aldrich, St. Louis, MO) was mixed with PBS at a concentration of 5 mg/ml and sonicated for 20 min to create a homogenous suspension. The suspension was autoclaved, allowed to cool to room temperature and re-sonicated for 20 min immediately before injection. Mice were i.p. injected with 800 µl of the carbon suspension. At 14 days post injection (dpi) mice were euthanized. Omenta were harvested and fixed in 10% formalin for 2 hrs at room temperature. Whole fixed tissue was dehydrated through increasing concentrations of ethanol (i.e. 70%, 90% and 2x 100%; 10 min each) and cleared in xylenes for 10 min. Finally, tissues were whole-mounted between a slide and coverslip using Permount. Images of the whole-mounted tissues were captured using a CRi Pannoramic Scan Whole Slide Scanner in the University of Chicago Light Microscopy Core Facility and images were processed with Pannoramic Viewer software (3D Histech, Budapest, Hungary).

Milky Spot Identification Using Giemsa Staining: Excised omenta were prepared for standard histologic evaluation, with careful orientation of the tissues while paraffin embedding to produce longitudinal sections. The whole omentum was serially sectioned (4 µm) and every third section was Giemsa stained (Fluka, St. Louis, MO). Slides were deparaffinized in xylenes and rehydrated through serial dilutions of ethanol to water. Slides were stained in 5% Giemsa solution (prepared in tap water) for 4 min, rinsed in tap water for 60 sec, allowed to air-dry and coverslipped using Permount. Images of the stained slides were captured using a CRi Pannoramic Scan Whole Slide Scanner in the University of Chicago Light Microscopy Core Facility and images were processed with Pannoramic Viewer software (3D Histech, Budapest, Hungary).

Three-Dimensional Rendering of Giemsa-Stained Omentum: ImageJ software was used to render a three-dimensional image of a B6 omentum. Imaged, Giemsa-stained omentum sections from an entire omentum were aligned using the StackReg plugin.[51] The resulting

277 stack was Inverted and the 3D Project tool, with the interpolate function set to a slide spacing
278 of 4 μm, was used to render a three-dimensional image. This was converted to 8-bit
279 grayscale and false-colored using the Unionjack color scheme.

280 **Milky Spot Identification and Quantitation in Giemsa-Stained Omenta:** ImageJ software
281 was used to quantify the milky spot volume in the Giemsa-stained omental sections. Images
282 were converted to 8-bit grayscale and Inverted. The Color Balance was adjusted to increase
283 the contrast between the milky spots and surrounding tissue. The image was converted to
284 Binary to reduce background and Inverted again. The Threshold was set using the Auto
285 function, resulting in an image where milky spots are pure black and the rest of the tissue is
286 pure white. The resulting immune aggregates were measured using the Analyze Particles
287 function. This was repeated for each of the Giemsa-stained sections per omentum. Milky spot
288 areas for each omentum section were multiplied by 4 μm and summed to produce a total
289 milky spot volume. The whole omentum volume was measured by adjusting the
290 Brightness/Contrast of a grayscale image to darken the immune aggregates. The Threshold
291 was set to include the entire tissue and the image was converted to a pure black Mask. To
292 create a cohesive border for the omentum, the Find Edges tool was applied and the image
293 was again converted to a Mask and Fill Holes was selected. Again, the omentum was
294 quantified using the Analyze Particle function. Particles smaller than 25 pixels were excluded
295 in the analysis to reduce any background noise. Areas for each omentum were multiplied by
296 4 μm and summed to produce a total whole omentum volume. Macros of the above image
297 processing steps are available as Supplemental Methods. n=5 omenta per each mouse
298 strain.

299 **Quantitation of Adipocyte Area in Omenta Over the Timecourse of Metastatic**
300 **Colonization.** Omenta were harvested from mice at 1, 3, 6 and 9 weeks after cancer cell

injection and tissues were prepared for standard histologic evaluation. H&E-stained sections were imaged using a CRi Pannoramic Scan Whole Slide Scanner. Using ImageJ, section images were converted to 8-bit grayscale, the Brightness/Contrast was adjusted to darken the non-adipocyte tissue and the image Threshold was set (using the Auto function) such that only non-adipocyte structures were transformed to pure black. These structures were measured using the Analyze Particles function with particles smaller than 25 pixels excluded. Resulting areas were summed to produce a total non-adipocyte area. The whole omentum was measured by adjusting the Threshold of a Brightness/Contrast-adjusted grayscale image such that the whole area is converted to pure black. Again, the omentum was quantified using the Analyze Particle function excluding particles smaller than 25 pixels with the Include Holes option selected. Resulting areas were summed to produce a total omentum area. The percentage of adipocytes was calculated by subtracting the total non-adipocyte area from the total omentum area and dividing that by the total omentum area. Macros of the above image processing steps are available as Supplemental Methods. A total of three sections were quantified per mouse with n=5 mice per timepoint.

Statistics: All statistical analyses were performed using GraphPad Prism (GraphPad Software, La Jolla, CA). Data was presented as mean of biologic replicates. All error bars represent statistical error of the mean. Statistical significance was determined using one-way analysis of variance (ANOVA) followed by Tukey-Kramer multiple comparison tests. One, two and three asterisks represent $p<0.05$, $p<0.01$, $p<0.001$, respectively.

Results

Several sources of adipose tissue are accessible to ovarian cancer cells in the peritoneal cavity. The organ-specificity of ovarian cancer metastasis is often explained by the omentum's anatomic location and tissue composition.[6,46] However, to our knowledge,

these assertions have not been tested *in vivo* by evaluating ovarian cancer cell lodging or growth in other adipose depots that are accessible during peritoneal dissemination. There are five major adipose-rich structures in the peritoneal cavity.[3] As shown in Figure 1A, a lateral view of a ventral dissection allows visualization of the omentum (OM), gonadal fat (GF), uterine fat (UF) and mesentery (MY). The ovary (ov), uterine horn (uh) and small intestine (si) are indicated as points of reference. Further dissection allows for clear visualization of the splenoportal fat (SP), which connects the hilum of the spleen to the pancreas (Figure 1B), and the omentum, shown isolated from the pancreas (Figure 1C). The gross structure and relative size of these tissues is shown in Figure 1D. Interestingly, it has been reported that the splenoportal fat contains milky spots that are analogous to omental milky spots in both composition and structure.[48] In agreement with these published findings, histologic evaluation of tissues confirmed the presence milky spots in the omentum and splenoportal fat and the absence of milky spots in uterine and gonadal fat (Supplemental Figure S1). In the case of the mesentery, our findings differed somewhat from the literature[52] as we only observed occasional minute clusters of lymphoid cells which were smaller and less structurally distinct than the milky spots seen in omental and splenoportal fat (Supplemental Figure S1). Taken together these data show that during peritoneal dissemination, ovarian cancer cells have access to and can interact with adipose tissues that either contain or lack milky spot structures.

Ovarian cancer cells only colonize peritoneal adipose that contains milky spots. As described in the introduction, a review of the literature showed that ovarian cancer's predilection for omental metastasis formation can be ascribed to either adipose-driven or milky spot-driven mechanisms. However, these models were prompted by reductionist studies focusing on either structural features (i.e. milky spots) or cellular components (i.e.

adipocytes) of omental tissue.[30,44,47] The availability of peritoneal fat depots that contain or lack milky spot structures enabled us to experimentally distinguish between the two models in the physiologically relevant setting of the peritoneal cavity. We reasoned that if colonization were purely adipocyte-driven, ovarian cancer cells would colonize all of the peritoneal adipose depots after i.p. injection. In contrast, if milky spots were required for this process, only the omentum and splenoportal fat would be colonized. To test this, we assessed the lodging and growth of ID8 cancer cells on the five distinct peritoneal fat depots after i.p. injection into B6 mice. At 7 days post-injection (dpi), large colonies of ID8 cells were only seen within the milky spots of both the omentum and splenoportal fat (Figure 2A, left). No ovarian cancer cells were detected in the uterine or gonadal fat (Figure 2A, right). When the mesentery was examined, the rare lodged cancer cells seen were associated with the few immune aggregates present in that tissue (data not shown). Even at an assay endpoint (42 dpi) when animals have peritoneal disease burden that requires euthanasia, no ovarian cancer cells could be detected by histologic evaluation of the fatty tissues lacking milky spots (data not shown). As a confirmation of these findings, human SKOV3ip.1 cells were similarly injected into Nude mice. At 7 dpi large colonies of SKOV3ip.1 cells were observed in milky spots within the omentum and splenoportal fat (Figure 2B). Using IHC for human pan-cytokeratin, we confirmed that these lesions were composed of epithelial (SKOV3ip.1) cells intermingled with the immune cells. The specificity of staining was confirmed using an IgG control for the pan-cytokeratin antibody (Figure 2B).

Omental tissues secrete a factor(s) that can promote ovarian cancer cell migration. Ovarian cancer cells specifically localize to the omentum within minutes after i.p. injection.[4,7,42] This suggests that omental tissue produces a factor(s) that promotes cancer cell homing; however, previous studies have only examined the contribution of isolated

adipocytes.[47] To address this gap in knowledge, we first tested the ability of omentum-conditioned media to promote directed cancer cell migration. Using a modification of our published method for *ex vivo* organ culture,[7] omenta were excised and allowed to normalize in DMEM/F12 media containing 20% FCS for 24 hrs. Tissues were then rinsed with PBS, placed in serum-free DMEM/F12 and maintained for up to 5 days *ex vivo*. Tissue integrity was assessed both histologically by visually evaluating intact (round, continuous cell membrane) versus necrotic (stellate, discontinuous cell membrane) adipocytes and functionally by measuring the level of IL-6 in the conditioned media every 24 hrs. In agreement with our previously published studies,[7] omental tissues did not show loss of integrity or function under these conditions (Supplemental Figure S2, top row).

The experimental design used for the migration assays is summarized in Figure 3A. After normalization in DMEM/F12 containing 20% FCS, omenta were rinsed with PBS and allowed to condition serum-free DMEM/F12 for 24 hrs (subsequently referred to as conditioned serum-free media; CSF). Omenta maintained in serum-free (SF) media are termed starved omenta (SOM). The combinations of omenta and media used as chemoattractants for the 6 hr migration assay are summarized in Figure 3B, upper panel, while representative membranes from the migration assays are shown in Figure 3B, lower panel. The number of cells that migrated to the lower side of the membrane was determined by summing the number of cells in each of 5 independent fields observed at 100x magnification.

Initial studies tested the ability of omenta harvested from CD1 mice to promote migration of both mouse ID8 and human SKOV3ip.1 cells (Figure 3C). With both cell types, the combination of SF media and SOM during the 6hr migration assay caused small, yet reproducible, stimulation of migration above that seen in the SF media controls. In contrast, CSF media served as a strong chemoattractant for both ID8 and SKOV3ip.1 cells, resulting in

a greater than 150-fold increase in migration relative to SF media controls. The addition of SOM to the CSF media (CSF+SOM) did not further enhance cell migration. To ensure that these results are not specific to omenta harvested from CD1 mice, CSF from B6 and Nude mice were also tested in their ability to promote ID8 and SKOV3ip.1 cell migration. As shown in Figure 3D, migration of ID8 and SKOV3ip.1 cells were statistically identical in response to conditioned media from both B6 and Nude omenta. Interestingly, ID8 cells show a consistently higher level of migration than SKOV3ip.1 cells in response to media conditioned by CD1, B6 and Nude mice. Taken together, these experiments showed that intact omental tissue can be used as a starting point for efforts to identify the secreted factor(s) that promote ovarian cancer cell homing to omental tissues.

Milky spot-containing tissues show enhanced ability to stimulate directed migration. In their work, Nieman *et al.* showed that adipocytes cultured *in vitro* secreted cytokines that can promote migration of SKOV3ip.1 ovarian cancer cells.[47] This raised the possibility that migration of cancer cells toward omentum-conditioned media could be a strictly adipose-driven process. If that were the case, we predicted that media conditioned by adipose tissue lacking milky spots would promote migration of ovarian cancer cells to the same extent as milky spot-containing adipose tissue. Alternatively, if milky spots are responsible for organ-specific homing, we expected that conditioned media from tissues containing milky spots could have an enhanced ability to promote migration. To distinguish between these possibilities, CSF media was prepared using weight-matched tissue equivalents of omentum, splenoportal fat, uterine fat and mesentery and used as a chemoattractant in transwell migration assays. As shown in Supplemental Figure S2, tissues did not show loss of integrity or function for the duration of the migration assay. However, it was noted that the IL-6 production of the cultured uterine fat dropped significantly at 3 days in culture (Supplemental

Figure S2). The migration-promoting activity of CSF prepared from each of these tissues is summarized in Figure 3E. Media conditioned by omenta and splenoportal fat caused a 95-fold increase in cell migration as compared to SF media controls. In contrast, the absence of milky spots in uterine fat and mesentery corresponded with 75% reduction in the migration-stimulatory activity in their conditioned media (Figure 3E). Taken together, these functional studies bridge the adipocyte-driven and milky spot-driven models and argue that the presence of milky spots increases the chemoattractive potential of peritoneal fat depots.

The number and size of omental milky spots is not dependent on the mouse genetic background. Immune cells, including macrophages, lymphocytes and mast cells, are integral to both the composition and function of omental milky spots.[31,36,39,41] This raised the question, "Are specific immune cell types required for milky spot formation, maintenance and function?" As a first step toward answering this question, we tested the possibility that mutations depleting or inactivating specific lymphocyte populations (i.e. immunodeficient mouse models) could affect the number and size of omental milky spots. The majority of published studies use two standard methods to identify milky spots. The first employs a nonspecific esterase stain, which colors macrophages and T-lymphocytes dark red.[31] In our hands, this method yielded highly variable results that were not of sufficient quality or resolution for quantitative analyses (data not shown). A second method employs i.p. injection of a carbon nanopowder suspension, which is phagocytosed by peritoneal macrophages over a period of days.[31] Tissues are subsequently harvested, whole-mounted and the number and/or area of the black-staining macrophages are used as a measure of milky spot number and size. When this method works correctly the milky spot structures are crisp and well defined, and they can be visualized and counted under light microscopy (Figure 4A). However, we found that this technique can give inconsistent results because carbon plaques (indicated by arrows) often

form on various peritoneal surfaces (Figure 4B). This plaque formation prevents both precise isolation (excision) of the omentum and accurate evaluation of milky spot area in the whole-mounted tissue.

To circumvent this problem, we developed a novel technique to visualize the milky spots on a whole-mount scale using Giemsa staining. In this approach, excised omenta were paraffin-embedded and the entire organ serially sectioned at 4 µm (resulting in ~30-60 sections). Every third section was stained in a 5% Giemsa solution and images of the stained tissues captured using a CRi Pannoramic Scan Whole Slide Scanner (Figure 4C). As shown in Figure 4D, milky spots appear as dark blue-staining areas. The identity of these regions as milky spots was confirmed in serial sections by both H&E staining and IHC for CD45+ (Cluster of Differentiation 45; common lymphocyte marker) cells (Figures 4E and 4F, respectively). Milky spots from B6, Nude, Rag1, Igh6 and BN XID mice were successfully stained with Giemsa using this method (Supplemental Figure S3). By stacking and aligning all of the Giemsa stained images from one omentum, we were able to produce a three-dimensional rendering of a mouse omentum that accurately depicts the tissue architecture and presents a novel view of the location and structure of milky spots (Supplemental Video S4).

We used ImageJ to process the Giemsa-stained omentum slices in order to produce images that display both milky spots (Figure 4G) and the whole omentum area (Figure 4H) as pure black pixels (the processing steps are detailed in the Materials and Methods section). These black pixels were quantified using the Analyze Particle feature of ImageJ producing a milky spot area and a whole omentum area for each slice. Since each section was cut at 4 µm, those areas were summed and multiplied by 4 µm to produce milky spot and total volume for each omentum. Surprisingly, we found no difference among the milky spot volumes

(Figure 5A) or the omentum volumes (Figure 5B) for the 5 mouse strains. Furthermore, no significant difference was found when the milky spot volume was expressed as a percentage of the total omentum area (Figure 5C). These data show that the volume of milky spots present in the omentum is not affected by deficiency or absence of T cells, B cells or NK cells in these well-established immune-competent and immunodeficient mouse strains.

***In vivo* colonization of omental milky spots by ovarian cancer cells is not dependent on their immune cell composition.** As a first step toward understanding the effect of the immune cell composition of milky spot structures on ovarian cancer cell colonization, experimental metastasis assays were conducted using our panel of immune competent and deficient mice. Specifically, 1 x 10^6 ID8 ovarian cancer cells were injected i.p. into syngeneic B6 mice. In parallel, 1 x 10^6 SKOV3ip.1 human ovarian cancer cells were injected into Nude, Rag1 and BN XID mice. Cancer cell foci were observed within milky spots in each of these mouse strains at 7 dpi (Figure 6A). To confirm that the infiltrating cells were in fact SKOV3ip.1, we stained relevant sections for epithelial pan-cytokeratin. SKOV3ip.1 lesions were cytokeratin-positive (Figure 6B) with no discernable background staining in the IgG control for the pan-cytokeratin antibody or PBS-injected control mice. Thus, ovarian cancer cell colonization of omental milky spots is not affected by deficiency or absence of T cells, B cells or NK cells in these mouse strains.

During progressive growth ovarian cancer cells replace omental adipose. Mechanistic studies by Nieman *et al*. indicated that ovarian cancer cells could use adipocytes as an energy source for tumor growth.[47] If this holds true *in vivo*, we predicted that as cancer cells proliferate, they interact with and consume adipocyte lipids. The ultimate outcome of this inverse relationship between cancer cell area and adipocyte area would be that, at the experimental endpoint, the omental adipose would be replaced completely with cancerous

493 tissue. To test this notion, 1 x 10^6 ID8 ovarian cancer cells were injected i.p. into a cohort of
494 B6 mice. Groups of 5 mice were euthanized and tissues collected for histologic analysis at 1,
495 3, 6 and 9 weeks post injection (Figure 7A). Consistent with an inverse relationship between
496 ovarian cancer cell growth and adipocyte depletion, there is a marked reduction in the
497 adipocyte area over time. To quantify this change, we used an image processing protocol
498 similar to milky spot quantification (detailed in the Materials and Methods) to produce images
499 that show all non-adipocyte areas as pure black pixels as well as the total omentum area as
500 pure black pixels. Those pixels were quantitated in three separate sections per mouse and
501 showed a linear decrease in the percentage of adipocytes in the omentum corresponded to
502 the expansion of ID8 cancer cell lesions (Figure 7B). These data are consistent with cancer
503 cells' utilization of lipids stored in adipocytes as an energy source for their continued growth.

504 **Discussion**

505 There is now considerable literature on the structure and function of milky spots in both the
506 omentum and extraomental sites. Beginning in the 1970s, investigators noted that ascites
507 tumors had a proclivity for these structures.[43] Subsequent studies confirmed and refined
508 these findings.[4,7,42] The strength of this work is that it implies a functional role for milky spots
509 in the early steps of omental colonization. However, the weakness of the "milky spot-driven"
510 model prompted by this body of literature is that the studies on which it is based do not
511 consider the potential contribution(s) of adipocytes and other cells within the adipose-rich
512 region. While the failure to consider the contribution of omental adipose in cancer metastasis
513 is consistent with the now-antiquated view of fat as an inert component of connective
514 tissues,[16,21,22] it is a fundamental oversight that must be addressed if we are to understand
515 the organ specificity of ovarian cancer cells.

In contrast, the adipocyte-driven model prompted by the findings of Nieman *et al.*, showed that in omental metastases, ovarian cancer cells at the interface with adipocytes contained abundant lipids.[47] *In vitro* studies showed that the adipocytes transfer lipid droplets that contain fatty acids that can be used as an energy source to ovarian cancer cells.[47] The strength of their studies is that they focused on human ovarian cancers and identified a novel function for adipocytes in the progressive growth of ovarian cancer lesions. The weakness of this work lays in its effort to show that adipocytes drive, and are solely responsible for, early steps in omental colonization. The case for adipose as the sole determinant of the ovarian cancer's organotropic metastasis was based on an incomplete examination of the literature and a biased approach to experimental design. As a result of the focus on adipocytes, important clues in the data were overlooked and the potential contributions of milky spots, vasculature or other unique characteristics of the omentum were neither tested nor discussed. Thus, like the milky spot-driven model, this model is also limited by the reductionist studies upon which it was based.

Despite their strengths, neither the milky spot-driven nor the adipocyte-driven models address the intimate and dynamic interactions among milky spot structures, adipocytes and other components of the adipose-rich areas. Studies herein bridge and organize findings from both the milky spot- and adipocyte-driven models into a coherent model of omental colonization. Our data show that gonadal fat, uterine fat and mesentery secrete a factor(s) that promotes directed migration; however, results from *in vivo* assays show that ovarian cancer cells do not colonize these tissues. This suggests that colonization requires additional chemotactic signals and/or tissue structures. In support of this notion, *in vivo* assays showed that ovarian cancer cells efficiently colonize milky spots in the splenoportal fat (Figure 2). In addition, media conditioned by adipose containing milky spot structures showed significant

enhancement in its ability to promote directed cancer migration. After lodging within milky spot structures, ovarian cancer cells begin to proliferate. Finally, the role of adipocytes in supplying energy for cancer cells' growth is supported by the direct relationship between cancer cell growth and adipocyte depletion. These agree with breast cancer models where cancer growth causes a reduction in adipocyte number and size (reducing the adipocyte-to-cancer area ratio), implying lipolysis and possible adipocyte de-differentiation.[53]

Our finding that milky spots are required for colonization of peritoneal adipose confirms and extends previous work[4,7,26,30,42-46] and provides a foundation for studies to identify milky spot components involved in cancer cell homing and invasion. As a first step toward this goal, the use of immunodeficient mouse strains allowed us rule out a requirement for B cells, T cells or NK cells for ovarian cancer cell lodging within milky spots, confirming and expanding on the findings of Lotan *et al.*[9] Previous studies have shown that mast cells and macrophages are frequently observed in the milky spots.[32,35,36,38] Macrophages are an intriguing candidate as they can initiate the directed migration of disseminated mammary cells using secreted epidermal growth factor (EGF)[54] and have been shown to assist the survival and growth of established tumors.[55-57] Further, the depletion of peritoneal macrophages has been shown to decrease ovarian cancer tumor burden on the diaphragm at the experimental endpoint.[58] Altogether, milky spot macrophages are potentially the source of the omentum's chemotactic properties and warrant future study.

Both the mesothelium and vasculature of milky spots may also contribute to milky spot colonization. A majority of studies support the notion that cancer cells exploit the stomata over the milky spots to gain access to the interior milky spot structures.[46,59] It is unclear whether the cancer cells simply push their way through the stomata during milky spot invasion[60] or if the mesothelial cells surrounding the stomata actively assist in the localization

process by secreting a chemotactic factor.[30,44] Similarly, endothelial cells within the highly fenestrated capillaries of the omental glomeruli may play a role in promoting cancer cell migration to and subsequent growth within milky spot structures. For example, previous studies have shown that VEGF-A produced by endothelial cells promotes the directed migration of breast cancer cell.[61] Furthermore, endothelial cells can secrete IL-6, CXCL8 and EGF to stimulate migration and anoikis resistance of head and neck squamous cell carcinoma.[62] In fact, the dense capillary network may promote cancer progression in that high tumor microvessel density can negatively predict ovarian cancer survival.[63] Taken together, these attributes also make endothelial cells excellent candidates as primary promoters of metastatic tumor growth at the omentum.

While we found that milky spot structures are necessary for colonization, the literature indicates that they may not be sufficient for colonization. Studies indicate that these structures are also present in other serous membranes including the pleural mesothelium, a site where we do not observe ovarian cancer cells in *in vivo* assays.[26,48,64] This suggests that in addition to providing energy, adipocytes influence milky spot function. It is now well established that lipid droplets, such as those transferred to ovarian cancer cells,[47] are in fact highly-regulated organelles that can participate in cell activation and metabolism. The potential contribution(s) of lipid droplets to inflammatory and neoplastic processes is a subject of intense interest.[65] Of particular relevance to omental colonization, reports suggest that adipocytes and lymphoid cells interact in a paracrine manner giving the adipocytes properties that distinguish them from classical adipocytes.[26,66,67] Similarly, association with cancer cells results in dysfunctional adipocytes that overexpress adipokines and proteases that aid in tumor progression and colonization. For example, adipokines such as IL-6 and IL-8 may function as general chemoattractants that work in concert with additional factors that specify

588 milky spot localization.[47,53,68] Conversely, cancer cells primed by adipocytes can also show
589 increased migration and invasive potential.[53,69] For example, breast cancer cells treated with
590 adipocyte-conditioned media showed increased expression of immune cell-related genes,[70]
591 potentially contributing to the milieu of pro-inflammatory cytokines.

592 The growing emphasis on the role of the host tissue microenvironment in metastasis
593 formation stems from the seminal work of Stephen Paget showing that certain tumor cells
594 (the "seed") have a proclivity for specific organ microenvironment(s) (the "soil").[71-73] A
595 powerful, but often underappreciated, aspect of studies by Paget and other pioneers of
596 metastasis research was their innate appreciation of the unique tissue architecture,
597 physiology and function of the target organ that is essential to understanding metastatic
598 organ specificity.[74-77] The studies presented herein integrate milky spot and adipocyte
599 function in the context of the adipose-rich tissues of the omentum. We propose an integrated,
600 two-step model for omental colonization wherein the localization of disseminated cancer cells
601 is dependant upon milky spots. Adipocytes are subsequently required for progressive growth.
602 This model is likely a more accurate representation of the overall process of metastatic
603 colonization. It is our hope that both our findings and discussion of the larger literature will
604 serve as a framework for studies that will continue to refine our understanding of omental
605 colonization. Ultimately, it is our goal to use this information to extend the duration of
606 metastatic suppression.

607 **Acknowledgements**

608 We thank Mr. Nathan Stadick for his critical review of the literature, which contributed to the
609 scholarship of the manuscript. We also thank Dr. Erin Howe for her review and comments,
610 which greatly enhanced the discussion of our results. We are indebted to Ms. Shirley Bond
611 and Dr. Christine Labno, Technical Directors of the integrated microscopy core facility, for

612 their assistance and expertise in the capturing and quantification of the omentum images. We
613 also thank Ms. Terri Lee and Ms. Christy Schmehl of the Human Tissue Resource Center for
614 sectioning and staining of tissue samples.
615

References

1. Howlander N, Noone AM, Krapcho M, Neyman N, Aminou R, Waldron W, Altekruse SF, Kosary CL, Ruhl J, Tatalovich Z, Cho H, Mariotto A, Eisner MP, Lewis DR, Chen HS, Feuer EJ, Cronin KA, editors: SEER Cancer Statistics Review, 1973–2009 (Vinatage 2009 Populations) [Internet]. Bethesda, MD, National Cancer Institute, 2012 Apr. Available from: http://seer.cancer.gov/csr/1975_2009_pops09/
2. Naora H, Montell DJ: Ovarian Cancer Metastasis: Integrating insights from disparate model organisms. Nat Rev Cancer 2005, 5:355–366.
3. Cinti S: The Adipose Organ. Fantuzzi G, mazzone T, editors. Adipose Tissue and Adipokines in Health and Disease, Totowa, New Jersey, Humana Press, 2007, pp. 3–19.
4. Hagiwara A, Takahashi T, Sawai K, Taniguchi H, Shimotsuma M, Okano S, Sakakura C, Tsujimoto H, Osaki K, Sasaki S: Milky spots as the implantation site for malignant cells in peritoneal dissemination in mice. Cancer Research, AACR, 1993, 53:687.
5. Roby KF, Taylor CC, Sweetwood JP, Cheng Y, Pace JL, Tawfik O, Persons DL, Smith PG, Terranova PF: Development of a syngeneic mouse model for events related to ovarian cancer. Carcinogenesis 2000, 21:585–591.
6. Lengyel E: Ovarian Cancer Development and Metastasis. The American Journal of Pathology, American Society for Investigative Pathology, 2010, 177:1053–1064.
7. Khan SM, Funk HM, Thiolloy S, Lotan TL, Hickson J, Prins GS, Drew AF, Rinker-Schaeffer CW: In vitro metastatic colonization of human ovarian cancer cells to the omentum. Clin Exp Metastasis 2010, 27:185–196.
8. Kenny HA, Krausz T, Yamada SD, Lengyel E: Use of a novel 3D culture model to elucidate the role of mesothelial cells, fibroblasts and extra-cellular matrices on

adhesion and invasion of ovarian cancer cells to the omentum. Int J Cancer 2007, 121:1463–1472.

9. Lotan T, Hickson J, Souris J, Huo D, Taylor J, Li T, Otto K, Yamada SD, Macleod K, Rinker-Schaeffer CW: c-Jun NH2-terminal kinase activating kinase 1/mitogen-activated protein kinase kinase 4-mediated inhibition of SKOV3ip.1 ovarian cancer metastasis involves growth arrest and p21 up-regulation. Cancer Research 2008, 68:2166–2175.

10. Liebermann-Meffert D: The greater omentum. Anatomy, embryology, and surgical applications. Surg Clin North Am 2000, 80:275–93–xii.

11. Collins D, Hogan AM, O'Shea D, Winter DC: The omentum: anatomical, metabolic, and surgical aspects. J Gastrointest Surg 2009, 13:1138–1146.

12. Platell C, Cooper D, Papadimitriou JM, Hall JC: The omentum. World J Gastroenterol 2000, 6:169–176.

13. Goldsmith HS: The Omentum: Basic Research and Clinical Application. 1st ed. Goldsmith HS, editor. New York, Cine Med, Inc, 1990.

14. Fedorko ME, Hirsch JG: Studies on transport of macromolecules and small particles across mesothelial cells of the mouse omentum. I. Morphologic aspects. Exp Cell Res 1971, 69:113–127.

15. Wilkosz S, Ireland G, Khwaja N, Walker M, Butt R, Giorgio-Miller A, Herrick SE: A comparative study of the structure of human and murine greater omentum. Anat Embryol 2005, 209:251–261.

16. Wozniak SE, Gee LL, Wachtel MS, Frezza EE: Adipose Tissue: The New Endocrine Organ? A Review Article. Dig Dis Sci 2008, 54:1847–1856.

17. Trayhurn P, Beattie JH: Physiological role of adipose tissue: white adipose tissue as an endocrine and secretory organ. Proc Nutr Soc 2001, 60:329–339.

18. Hauner H: The new concept of adipose tissue function. Physiol Behav 2004, 83:653–

658.

19. Scherer PE: Adipose tissue: from lipid storage compartment to endocrine organ. Diabetes 2006, 55:1537–1545.

20. Kershaw EE, Flier JS: Adipose tissue as an endocrine organ. J Clin Endocrinol Metab 2004, 89:2548–2556.

21. Wang P, Mariman E, Renes J, Keijer J: The secretory function of adipocytes in the physiology of white adipose tissue. J Cell Physiol 2008, 216:3–13.

22. Conde J, Scotece M, Gómez R, López V, Gómez-Reino JJ, Lago F, Gualillo O: Adipokines: biofactors from white adipose tissue. A complex hub among inflammation, metabolism, and immunity. Biofactors 2011, 37:413–420.

23. Frühbeck G, Gómez-Ambrosi J, Muruzábal FJ, Burrell MA: The adipocyte: a model for integration of endocrine and metabolic signaling in energy metabolism regulation. Am J Physiol Endocrinol Metab 2001, 280:E827–E847.

24. Tilg H, Moschen AR: Adipocytokines: mediators linking adipose tissue, inflammation and immunity. Nat Rev Immunol 2006, 6:772–783.

25. Rajala MW, Scherer PE: Minireview: The adipocyte--at the crossroads of energy homeostasis, inflammation, and atherosclerosis. Endocrinology 2003, 144:3765–3773.

26. Michailova KN, Usunoff KG: The milky spots of the peritoneum and pleura: structure, development and pathology. Biomedical Reviews, Varna, Bulgaria, 2004, 15:47–66.

27. Simer P: On the morphology of the omentum, with especial reference to its lymphatics. American Journal of Anatomy, Wiley Subscription Services, Inc., A Wiley Company, 1934, 54:203–228.

28. Ackermann PC, De Wet PD, Loots GP: Microcirculation of the rat omentum studied by means of corrosion casts. Acta Anat (Basel) 1991, 140:146–149.

29. Shimotsuma M, Shields J, Simpson-Morgan M, Sakuyama A, Shirasu M, Hagiwara A,

690 Takahashi T: Morpho-physiological function and role of omental milky spots as
691 omentum-associated lymphoid tissue (OALT) in the peritoneal cavity. Lymphology
692 1993, 26:90.
693 30. Gerber SA, Rybalko VY, Bigelow CE, Lugade AA, Foster TH, Frelinger JG, Lord EM:
694 Preferential Attachment of Peritoneal Tumor Metastases to Omental Immune
695 Aggregates and Possible Role of a Unique Vascular Microenvironment in Metastatic
696 Survival and Growth. The American Journal of Pathology, American Society for
697 Investigative Pathology, 2006, 169:1739–1752.
698 31. Shimotsuma M, Kawata M, Hagiwara A, Takahashi T: Milky spots in the human greater
699 omentum. Macroscopic and histological identification. Acta Anat (Basel) 1989,
700 136:211–216.
701 32. Shimotsuma M, Simpson-Morgan MW, Takahashi T, Hagiwara A: Activation of omental
702 milky spots and milky spot macrophages by intraperitoneal administration of a
703 streptococcal preparation, OK-432. Cancer Research 1992, 52:5400–5402.
704 33. Litbarg NO, Gudehithlu KP, Sethupathi P, Arruda JAL, Dunea G, Singh AK: Activated
705 omentum becomes rich in factors that promote healing and tissue regeneration. Cell
706 Tissue Res 2007, 328:487–497.
707 34. Rangel-Moreno J, Moyron-Quiroz JE, Carragher DM, Kusser K, Hartson L, Moquin A,
708 Randall TD: Omental Milky Spots Develop in the Absence of Lymphoid Tissue-Inducer
709 Cells and Support B and T Cell Responses to Peritoneal Antigens. Immunity, Elsevier
710 Ltd, 2009, 30:731–743.
711 35. Wijffels JF, Hendrickx RJ, Steenbergen JJ, Eestermans IL, Beelen RH: Milky spots in
712 the mouse omentum may play an important role in the origin of peritoneal
713 macrophages. Res Immunol 1992, 143:401–409.
714 36. Shimotsuma M, Takahashi T, Kawata M, Dux K: Cellular subsets of the milky spots in

715 the human greater omentum. Cell Tissue Res 1991, 264:599–601.
716 37. Cranshaw ML, Leak LV: Milky spots of the omentum: a source of peritoneal cells in the
717 normal and stimulated animal. Arch Histol Cytol 1990, 53 Suppl:165–177.
718 38. Beelen RH, Fluitsma DM, Hoefsmit EC: The cellular composition of omentum milky
719 spots and the ultrastructure of milky spot macrophages and reticulum cells. J
720 Reticuloendothel Soc 1980, 28:585–599.
721 39. Krist LF, Eestermans IL, Steenbergen JJ, Hoefsmit EC, Cuesta MA, Meyer S, Beelen
722 RH: Cellular composition of milky spots in the human greater omentum: an
723 immunochemical and ultrastructural study. Anat Rec 1995, 241:163–174.
724 40. Mironov VA, Gusev SA, Baradi AF: Mesothelial stomata overlying omental milky spots:
725 scanning electron microscopic study. Cell Tissue Res 1979, 201:327–330.
726 41. Dux K, Janik P, Szaniawska B: Kinetics of proliferation, cell differentiation, and IgM
727 secretion in the omental lymphoid organ of B10/Sn mice following intraperitoneal
728 immunization with sheep erythrocytes. Cellular Immunology, Elsevier, 1977, 32:97–
729 109.
730 42. Krist LF, Kerremans M, Broekhuis-Fluitsma DM, Eestermans IL, Meyer S, Beelen RH:
731 Milky spots in the greater omentum are predominant sites of local tumour cell
732 proliferation and accumulation in the peritoneal cavity. Cancer Immunol Immunother
733 1998, 47:205–212.
734 43. Green JA, Williams AE: The relationship between inflammatory responses and WBP1
735 tumour cell attachment to the rat omentum. Eur J Cancer 1978, 14:1153–1155.
736 44. Sorensen EW, Gerber SA, Sedlacek AL, Rybalko VY, Chan WM, Lord EM: Omental
737 immune aggregates and tumor metastasis within the peritoneal cavity. Immunol Res
738 2009, 45:185–194.
739 45. Tsujimoto H, Takhashi T, Hagiwara A, Shimotsuma M, Sakakura C, Osaki K, Sasaki S,

Shirasu M, Sakakibara T, Ohyama T: Site-specific implantation in the milky spots of malignant cells in peritoneal dissemination: immunohistochemical observation in mice inoculated intraperitoneally with bromodeoxyuridine-labelled cells. Br J Cancer, Nature Publishing Group, 1995, 71:468.

46. Tsujimoto H, Hagiwara A, Shimotsuma M, Sakakura C, Osaki K, Sasaki S, Ohyama T, Ohgaki M, Imanishi T, Yamazaki J, Takahashi T: Role of milky spots as selective implantation sites for malignant cells in peritoneal dissemination in mice. J Cancer Res Clin Oncol 1996, 122:590–595.

47. Nieman KM, Kenny HA, Penicka CV, Ladanyi A, Buell-Gutbrod R, Zillhardt MR, Romero IL, Carey MS, Mills GB, Hotamisligil GS, Yamada SD, Peter ME, Gwin K, Lengyel E: Adipocytes promote ovarian cancer metastasis and provide energy for rapid tumor growth. Nat Med 2011, 17:1498–1503.

48. Takemori N, Hirai K, Onodera R, Saito N, Namiki M: Light and electron microscope study of splenoportal milky spots in New Zealand black mice: comparison between splenoportal milky spots and aberrant spleens. J Anat 1995, 186 (Pt 2):287–299.

49. Yu D, Wolf JK, Scanlon M, Price JE, Hung MC: Enhanced c-erbB-2/neu expression in human ovarian cancer cells correlates with more severe malignancy that can be suppressed by E1A. Cancer Research 1993, 53:891–898.

50. Delves P, Martin S, Burton D, Roitt I: Roitt's Essential Immunology. 11th ed. Wiley-Blackwell, 2006.

51. Thévenaz P, Ruttimann UE, Unser M: A pyramid approach to subpixel registration based on intensity. IEEE Trans Image Process 1998, 7:27–41.

52. Weinberg DF, Baldo-Correa E, Lenzi HL, Borojevic R: Schistosoma mansoni: peritoneal plasmacytogenesis and polypoid transformation of mesenteric milky spots in infected mice. Exp Parasitol 1992, 74:408–416.

765 53. Dirat B, Bochet L, Dabek M, Daviaud D, Dauvillier S, Majed B, Wang YY, Meulle A,
766 Salles B, Le Gonidec S, Garrido I, Escourrou G, Valet P, Muller C: Cancer-associated
767 adipocytes exhibit an activated phenotype and contribute to breast cancer invasion.
768 Cancer Research 2011, 71:2455–2465.
769 54. Wyckoff J, Wang W, Lin EY, Wang Y, Pixley F, Stanley ER, Graf T, Pollard JW, Segall
770 J, Condeelis J: A paracrine loop between tumor cells and macrophages is required for
771 tumor cell migration in mammary tumors. Cancer Research 2004, 64:7022–7029.
772 55. Qian B-Z, Pollard JW: Macrophage diversity enhances tumor progression and
773 metastasis. Cell 2010, 141:39–51.
774 56. Tlsty TD, Coussens LM: Tumor stroma and regulation of cancer development. Annu
775 Rev Pathol 2006, 1:119–150.
776 57. Coussens LM, Werb Z: Inflammation and cancer. Nature 2002, 420:860–867.
777 58. Robinson-Smith TM, Isaacsohn I, Mercer CA, Zhou M, Van Rooijen N, Husseinzadeh
778 N, McFarland-Mancini MM, Drew AF: Macrophages Mediate Inflammation-Enhanced
779 Metastasis of Ovarian Tumors in Mice. Cancer Research 2007, 67:5708–5716.
780 59. Barbolina MV, Moss NM, Westfall SD, Liu Y, Burkhalter RJ, Marga F, Forgacs G,
781 Hudson LG, Stack MS: Microenvironmental regulation of ovarian cancer metastasis.
782 Stack MS, Fishman DA, editors. Boston, MA, Springer US, 2009, pp. 319–334.
783 60. Iwanicki MP, Davidowitz RA, Ng MR, Besser A, Muranen T, Merritt M, Danuser G, Ince
784 T, Brugge JS: Ovarian Cancer Spheroids Use Myosin-Generated Force to Clear the
785 Mesothelium. Cancer Discovery 2011, 1:144–157.
786 61. Branco-Price C, Zhang N, Schnelle M, Evans C, Katschinski DM, Liao D, Ellies L,
787 Johnson RS: Endothelial cell HIF-1α and HIF-2α differentially regulate metastatic
788 success. Cancer Cell 2012, 21:52–65.
789 62. Neiva KG, Zhang Z, Miyazawa M, Warner KA, Karl E, Nör JE: Cross talk initiated by

endothelial cells enhances migration and inhibits anoikis of squamous cell carcinoma cells through STAT3/Akt/ERK signaling. Neoplasia 2009, 11:583–593.

63. H C Hollingsworth ECKSMSMLRMJM: Tumor angiogenesis in advanced stage ovarian carcinoma. The American Journal of Pathology, American Society for Investigative Pathology, 1995, 147:33.

64. Mixter RL: On macrophagal foci ("milky spots") in the pleura of different mammals, including man. American Journal of Anatomy, Wiley Online Library, 1941, 69:159–186.

65. Bozza PT, Viola J: Lipid droplets in inflammation and cancer. Prostaglandins 2010.

66. Pond CM: Adipose tissue: quartermaster to the lymph node garrisons. Biologist (London) 2000, 47:147–150.

67. Pond CM, Mattacks CA: Interactions between adipose tissue around lymph nodes and lymphoid cells in vitro. J Lipid Res 1995, 36:2219–2231.

68. Walter M, Liang S, Ghosh S, Hornsby PJ, Li R: Interleukin 6 secreted from adipose stromal cells promotes migration and invasion of breast cancer cells. Oncogene 2009, 28:2745–2755.

69. Tan J, Buache E, Chenard MP, Dali- Youcef N, Rio MC: Adipocyte is a non-trivial, dynamic partner of breast cancer cells. International journal of developmental biology, Departamento de Biología Celular e Histología, 2011, 55:851–859.

70. Kim JH, Kim K-Y, Jeon JH, Lee SH, Hwang J-E, Lee JH, Kim KK, Lim J-S, Kim KI, Moon E-Y, Lee HG, Ryu J-H, Yang Y: Adipocyte culture medium stimulates production of macrophage inhibitory cytokine 1 in MDA-MB-231 cells. Cancer Lett 2008, 261:253–262.

71. Paget S: The distribution of secondary growths in cancer of the breast. 1889. The Lancet 1889, 133:571–573.

72. Kenny PA, Bissell MJ: Tumor reversion: correction of malignant behavior by

microenvironmental cues. Int J Cancer 2003, 107:688–695.

73. Bissell MJ, Radisky DC, Rizki A, Weaver VM, Petersen OW: The organizing principle: microenvironmental influences in the normal and malignant breast. Differentiation 2002, 70:537–546.

74. Nicolson GL: Organ specificity of tumor metastasis: role of preferential adhesion, invasion and growth of malignant cells at specific secondary sites. Cancer Metastasis Rev 1988, 7:143–188.

75. Fidler IJ: The pathogenesis of cancer metastasis: the “seed and soil” hypothesis revisited. Nat. Rev. Cancer. 2003, pp. 453–458.

76. Hart IR, Fidler IJ: Role of Organ Selectivity in the Determination of Metastatic Patterns of B16 Melanoma. Cancer Research 1980.

77. Sugarbaker EV: Cancer metastasis: a product of tumor-host interactions. Curr Probl Cancer 1979, 3:1–59.

Figure Legends

Figure 1. The relative locations of the main depots of peritoneal adipose. A: Left view of the peritoneal cavity of a B6 mouse, exposed via a ventral incision. This gross anatomic dissection shows the relative location of four of the five primary sources of peritoneal fat. Beginning at the top center and moving clockwise are: the omentum (OM; outlined) located over the stomach and spleen, the gonadal fat (GF) surrounding the left ovary (ov), the uterine fat (UF) attached to the uterine horns (uh) and the mesentery (MY) attached to the small intestine (si). **B:** The fifth source of peritoneal adipose is the splenoportal fat, which can be exposed by lifting the spleen with forceps (SP; outlined). **C:** The mouse omentum shown dissected free from the pancreas and exposed here to improve visualization. Although analogous to the human omentum in composition and tissue architecture, in mice the omentum consists of a single ribbon of fat attached to the pancreas. **D:** Five sources of peritoneal fat excised to show relative size. From left to right: splenoportal fat, omentum, gonadal fat, uterine fat and mesentery (with attached mesenteric root).

Figure 2. Ovarian cancer cells specifically colonize peritoneal adipose that contains milky spots. A: B6 mice were injected i.p. with either PBS as a control (*upper panels*) or $1x10^6$ ID8 murine ovarian cancer cells (*lower panels*). At 7 dpi, tissues were excised for histologic evaluation. In control tissues (*upper panels*) milky spots (MS) are seen interspersed among adipocytes (A) in the omental and splenoportal fat. In contrast, no milky spots were detected in the uterine fat, gonadal fat and mesentery, each composed mostly of adipocytes (with occasional vessels being observed). After ID8 cell injection (*lower panels*), large foci of cancer cells intermixed with immune cells were observed within milky spots in the omentum and splenoportal fat (outlined in yellow). In contrast, ID8 cancer cells were not observed in the uterine fat, gonadal fat or mesentery. The scale bar is the same for all

images and denotes 50 μm. **B:** Nude mice were injected i.p. with $1x10^6$ SKOV3ip.1 human ovarian cancer cells. At 7dpi, omenta and splenoportal fat were excised for histological evaluation. Sections were evaluated by H&E staining. The presence of epithelial (cancer) cells within the lesions was confirmed by IHC detection of cytokeratin using a pan-cytokeratin antibody. IHC using an IgG isotype antibody for pan-cytokeratin was used as a control for staining specificity. The scale bar is the same for all images and denotes 100 μm.

Figure 3. Milky spot-containing adipose tissues show enhanced ability to stimulate directed migration. Transwell migration assays were used to test the ability of the omentum and other peritoneal adipose tissues to produce soluble factors that promote the directed migration of ovarian cancer cells. **A:** Schematic description of experimental design. **B:** *Top:* Depiction of migration assay setup. Cancer cells were placed in the upper chamber of the transwell apparatus. The chemoattractant media, with or without starved tissue, was placed in the lower chamber as indicated. *Bottom:* Representative membranes from ID8 migration assays. **C:** Quantitation of ID8 (*left*) and SKOV3ip.1 (*right*) cell migration in response to factors produced by omenta harvested from CD-1 mice. Conditions are those illustrated in Panel B, where SF denotes serum free media where CSF denotes conditioned serum and SOM denotes starved omentum. **D:** Quantitation of ID8 (*left*) and SKOV3ip.1 (*right*) cell migration in response to factors produced by omenta harvested from B6 and Nude mice. **E:** Migration assay of ID8 cells toward serum-free media conditioned for 24 hr by tissue equivalents of omenta (OM), splenoportal fat (SP), uterine fat (UF) and mesentery (MY) harvested from B6 mice. n=5 for all conditions. *$p<0.05$, ***$p<0.001$.

Figure 4. An alternative protocol for labeling milky spots in mouse omenta. A: A rare example of a whole mount of a B6 omentum with clear milky spot labeling after carbon staining. Scale bar = 1.0 mm. **B:** A more typical case of a B6 omentum ineffectively stained

878 with several carbon plaques (red arrows) obstructing milky spot visualization. Scale bar = 1.0
879 mm. **C:** As an alternative to carbon labeling, we developed a method wherein naive mouse
880 omenta were paraffin-embedded, sectioned at 4μm and stained with Giemsa. Dark staining
881 regions denote dense areas of immune aggregates. **D:** Image of omental tissue section
882 stained with Giemsa. Milky spots are indicated with black arrows. **E:** Image of omental tissue
883 section adjacent to D, stained with H&E. **F:** Image of omental tissue section adjacent to E,
884 evaluated by IHC using anti-CD45 antibody to identify lymphocytes within the milky spot
885 structure. The scale bar is the same for D-F and denotes 100 μm. **G:** Mask of omentum
886 section (same as C) processed to show milky spots specifically converted to pure black
887 pixels. **H:** Mask of omentum section (same as C) processed to show the entire area of the
888 omentum converted to pure black pixels. The scale bare is the same for C, G and H and
889 denotes = 1.0 mm.

890 **Figure 5. The milky spot volume of the omentum is not affected to the host's immune**
891 **status.** Giemsa-stained sections of omenta harvested from B6, Nude, Rag1, Igh6 and BN
892 XID mice were processed, sectioned, Geimsa stained and imaged to allow for automated
893 quantitation of milky spot and whole omenta area on each section (as described in the
894 Materials and Methods). Volumes were calculated by multiplying the area of each section by
895 4μm and summing sections from individual omenta. **A:** Milky spot volume per omentum. **B:**
896 Total volume of the whole omentum. **C:** Milky spot volume as a percentage of the total
897 omentum volume. For each mouse strain, milky spot and omental volumes were determined
898 for 5 independent animals. Using one-way ANOVA, no measurements were statistically
899 different among any of the mouse strains.

900 **Figure 6. Colonization of omental milky spots by ovarian cancer cells is not dependent**
901 **on the host immune status. A:** To test the possibility that the lymphocyte population of the

902 milky spots has a quantitative effect on ovarian cancer cell colonization, mice with
903 deficiencies in T cells, B cells and/or NK cells were injected i.p. with either PBS (control;
904 *upper panel*) or $1x10^6$ ovarian cancer cells (*lower panel*). B6 mice were injected with
905 syngeneic ID8 cells. Nude, Rag1 and BN XID mice were injected with human SKOV3ip.1
906 cells. Omenta were collected at 7 dpi and were processed for histology (using H&E staining).
907 Cancer cell foci within immune aggregates are outlined. The scale bar is the same for all
908 images and denotes 50 µm. **B:** IHC with a pan-cytokeratin antibody was used to confirm that
909 the lesions observed in milky spots of Nude, Rag1 and BN XID mice at 7 dpi were composed
910 of SKOV3ip.1 cells, tissue sections were immunostained with pan-cytokeratin antibody. As a
911 control for nonspecific background staining, omental tissue from Nude mice injected with PBS
912 was also evaluated by IHC using a pan-cytokeratin antibody (*far left panel*). To control for
913 antibody specificity, IHC with an isotype IgG for the pan-Cytokeratin antibody was used to
914 evaluate omental tissues from mice injected with SKOV3ip.1 cells. Samples from 5
915 independent animals were evaluated for each condition. The scale bar is the same for all
916 images and denotes 100 µm.

917 **Figure 7. Adipocyte area of the omentum decreases during the timecourse ovarian**
918 **cancer growth. A:** The first panel shows a representative H&E stained section of an
919 omentum from a naive B6 mouse. Milky spots are seen within adipose at the tissue
920 periphery. The four subsequent panels show representative images of omental tissues
921 harvested from B6 mice at 1, 3, 6 and 9 weeks post injection. The scale bar is the same for
922 all images and denotes 200 µm. **B:** Quantitation of adipocyte area from H&E images.
923 Reported values are percent adipocyte area normalized to whole omental area. Data at each
924 time point is based on five independent animals. A linear regression of the data points
925 indicates a slope significantly deviant from zero ($p<0.0001$) with $R^2 = 0.8145$.
926

Supplemental Figure 1. Representative histology of peritoneal fat deposits in naive B6 mice. Milky spots (MS) are seen at the tissue periphery adjacent to adipocytes (A) in the omentum and splenoportal fat of H&E stained tissue sections. Milky spots are not seen in H&E stained tissue sections from uterine fat, gonadal fat and mesentery. Arrows indicate blood vessels. The scale bar is the same for all images and denotes 50 μm.

Supplemental Figure 2. Evaluation of tissue integrity and function of tissues maintained in *ex vivo* culture. Left column: The effect of *ex vivo* culture on tissue integrity and cellularity was determined by histologic evaluation of freshly excised tissues. **Middle column:** Histology of tissues maintained for 24 hr in DMEM/F12 with 20% FCS followed by a 24 hr culture in DMEM/F12 with 20% FCS. **Right column:** To assess tissue viability and function under *ex vivo* conditions, the amount of IL-6 in the SF culture media was determined at 24 hr intervals. As a control, the amount of IL-6 secreted by tissues maintained in media containing 20% FCS was determined in parallel. The relative amount of IL-6 at each timepoint is the ratio of the measured IL-6 concentration to the IL-6 concentration in the control group. The scale bar is the same for all images and denotes 50 μm. ***$p<0.001$.

Supplemental Figure 3. Visualization of omental milky spots using Giemsa staining. Omenta from naive BL6, Nude, Rag1, Igh6 and BN XID mice were excised, sectioned and stained with Giemsa. **Left:** Whole omentum image, dark blue staining regions coincide with milky spot structures. **Right:** At higher magnification, milky spots are seen as dark-staining regions of immune cells.

Supplemental Figure 4. Three-dimensional rendering of mouse omentum. Giemsa stained sections of a naive B6 omentum were stacked, aligned and projected into a 3D rendering of the whole tissue. This false colored image depicts milky spots as white and stromal architecture as blue.

Supplemental Methods. Macros used for quantification of omental tissue components.

Milky Spot Area Quantification of Giemsa-Stained Tissue

```
run("8-bit");
run("Invert LUT");
run("Color Balance...");
setMinAndMax(146, 224);
call("ij.ImagePlus.setDefault16bitRange", 0);
run("Apply LUT", "stack");
run("Make Binary", " ");
run("Invert LUT");
setAutoThreshold("Default");
//run("Threshold...");
setThreshold(24, 255);
run("Convert to Mask", " ");
run("Analyze Particles...", "size=0-Infinity circularity=0.00-1.00 show=Masks display
summarize stack");
```

Omentum Area Quantification of Giemsa-Stained Tissue

```
run("8-bit");
//run("Brightness/Contrast...");
setMinAndMax(200, 255);
call("ij.ImagePlus.setDefault16bitRange", 0);
setAutoThreshold("Default");
//run("Threshold...");
setThreshold(0, 247);
setThreshold(0, 247);
run("Convert to Mask", " ");
run("Find Edges", "stack");
run("Convert to Mask", " ");
run("Convert to Mask", " ");
run("Fill Holes"," ");
run("Analyze Particles...", "size=25-Infinity circularity=0.00-1.00 show=Masks display include
summarize stack");
```

Non-Adipocyte Area Quantification of H&E-Stained Tissue

```
run("8-bit");
//run("Brightness/Contrast...");
setMinAndMax(161, 255);
call("ij.ImagePlus.setDefault16bitRange", 0);
//run("Threshold...");
setAutoThreshold("Default");
setThreshold(0, 195);
run("Analyze Particles...", "size=25-Infinity circularity=0.00-1.00 show=Masks display
summarize");
```

Omentum Area Quantification of H&E-Stained Tissue

```
run("8-bit");
```

```
999   //run("Brightness/Contrast...");
1000  setMinAndMax(243, 255);
1001  call("ij.ImagePlus.setDefault16bitRange", 0);
1002  setAutoThreshold("Default");
1003  //run("Threshold...");
1004  setThreshold(0, 248);
1005  run("Analyze Particles...", "size=25-Infinity circularity=0.00-1.00 show=Masks display include
1006  summarize");
1007
1008
```

Clark and Krishnan, *et al.* Figure 2

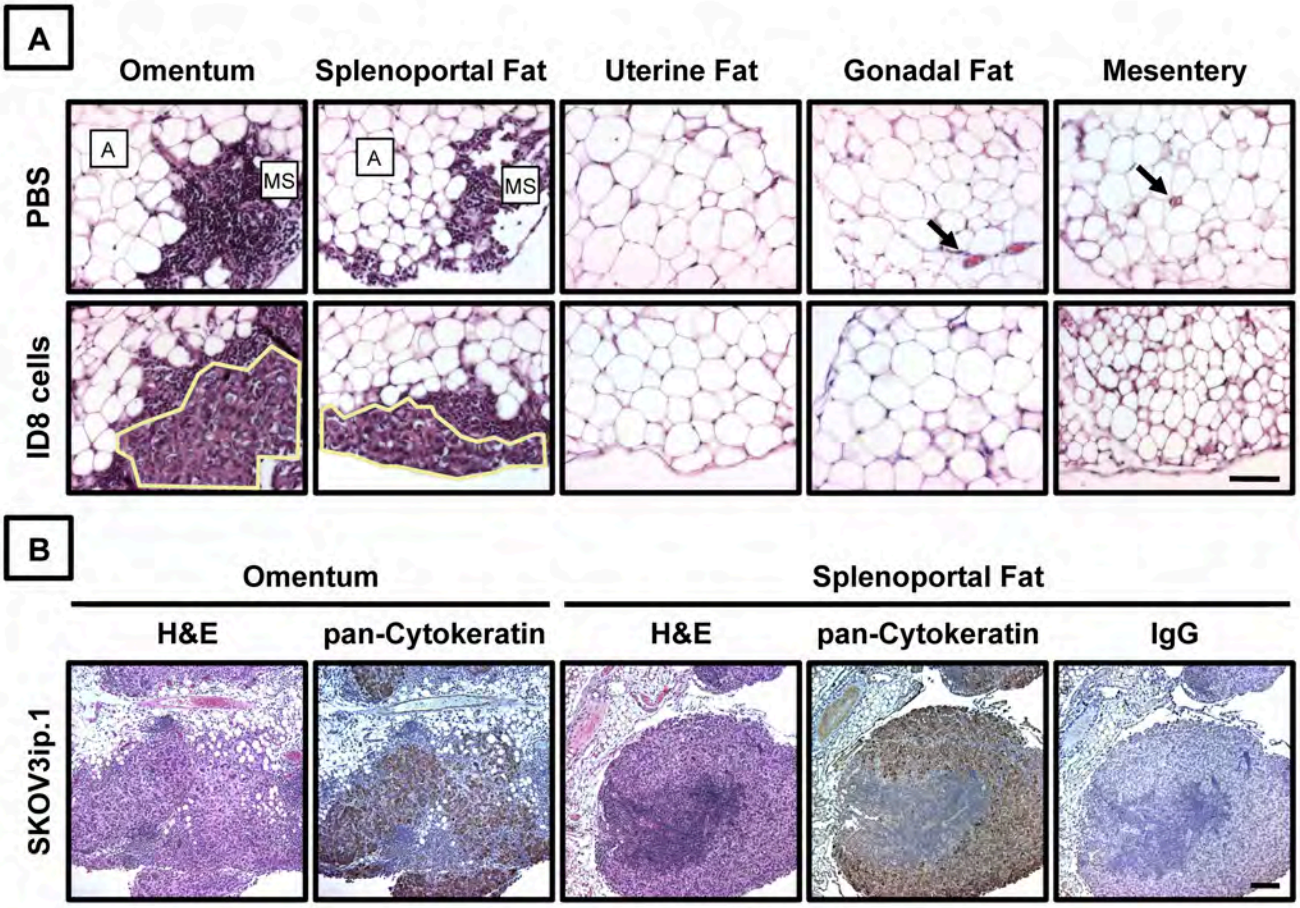

Clark and Krishnan, *et al*. Figure 3

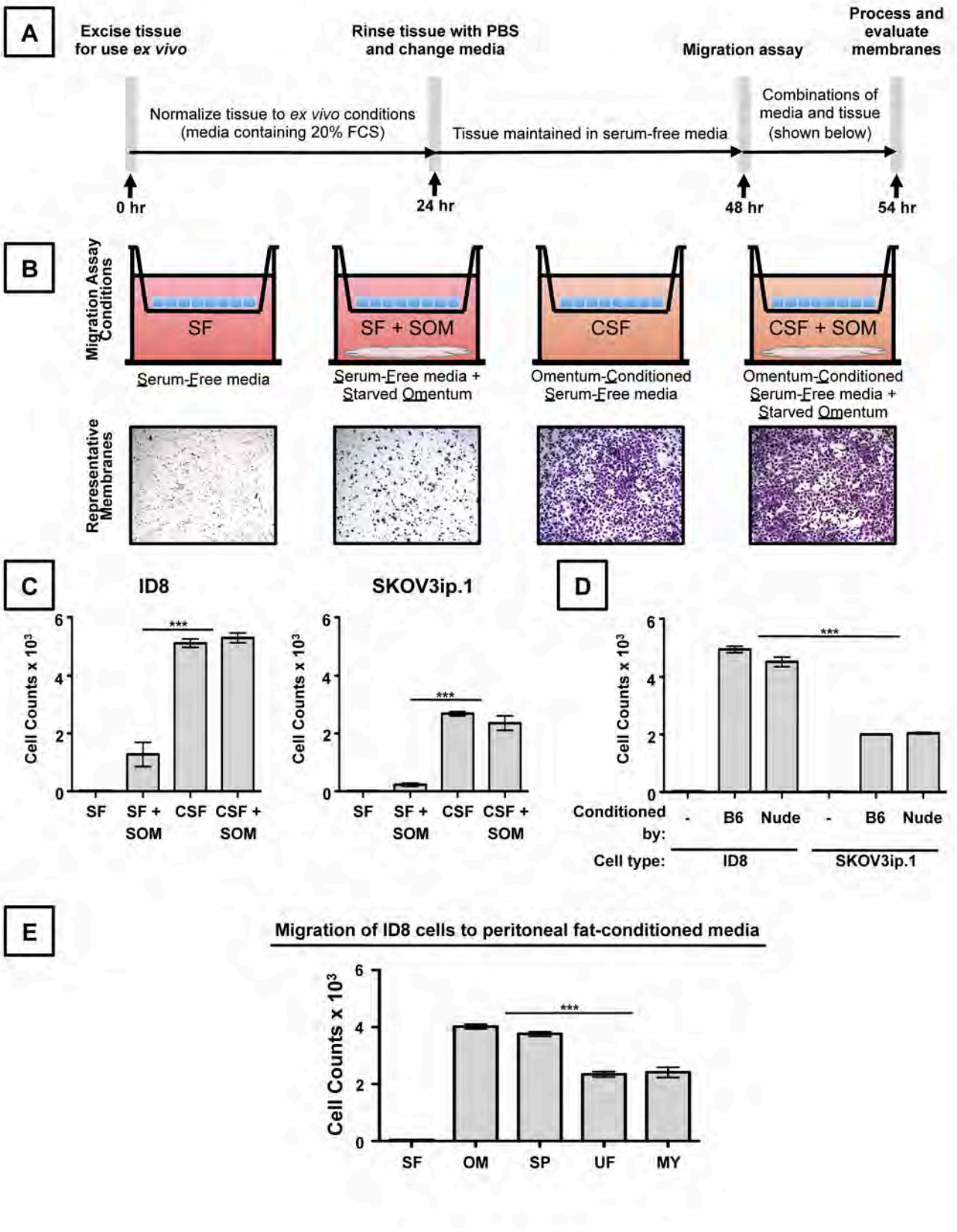

Clark and Krishnan, *et al*. Figure 4

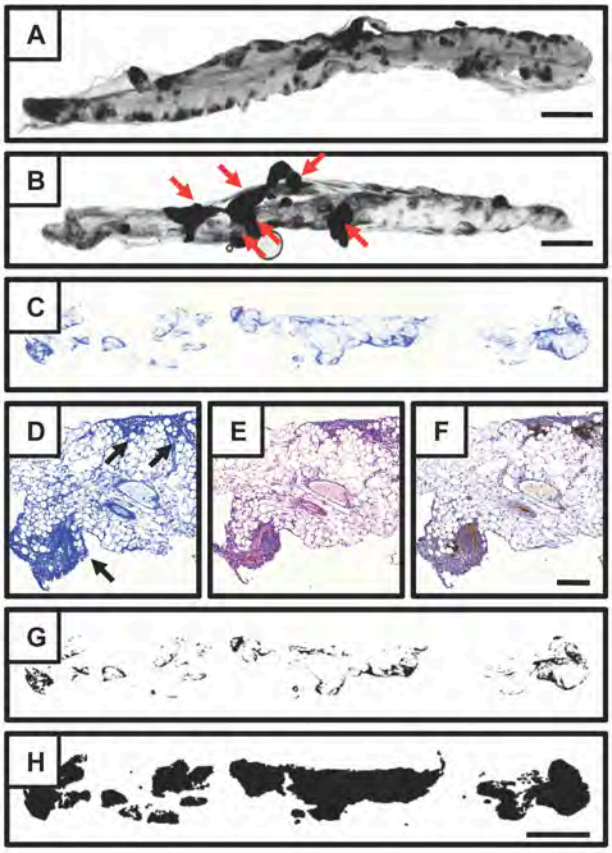

Clark and Krishnan, *et al*. Figure 5

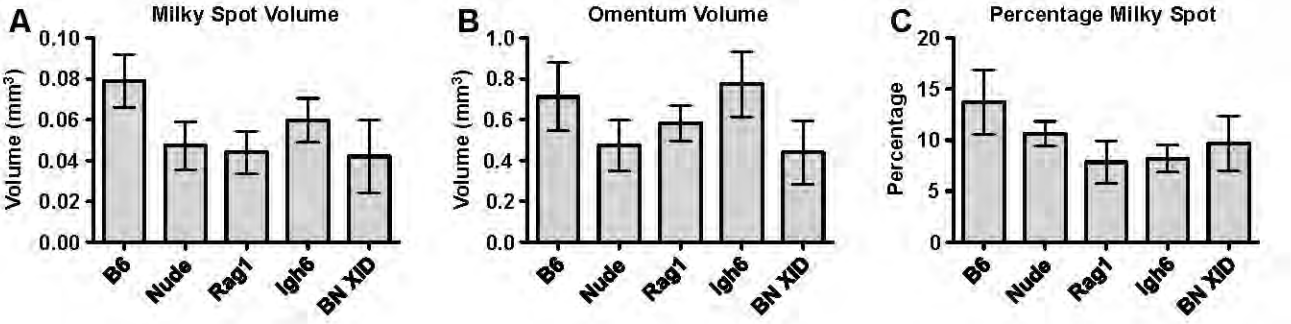

Clark and Krishnan, *et al.* Figure 6

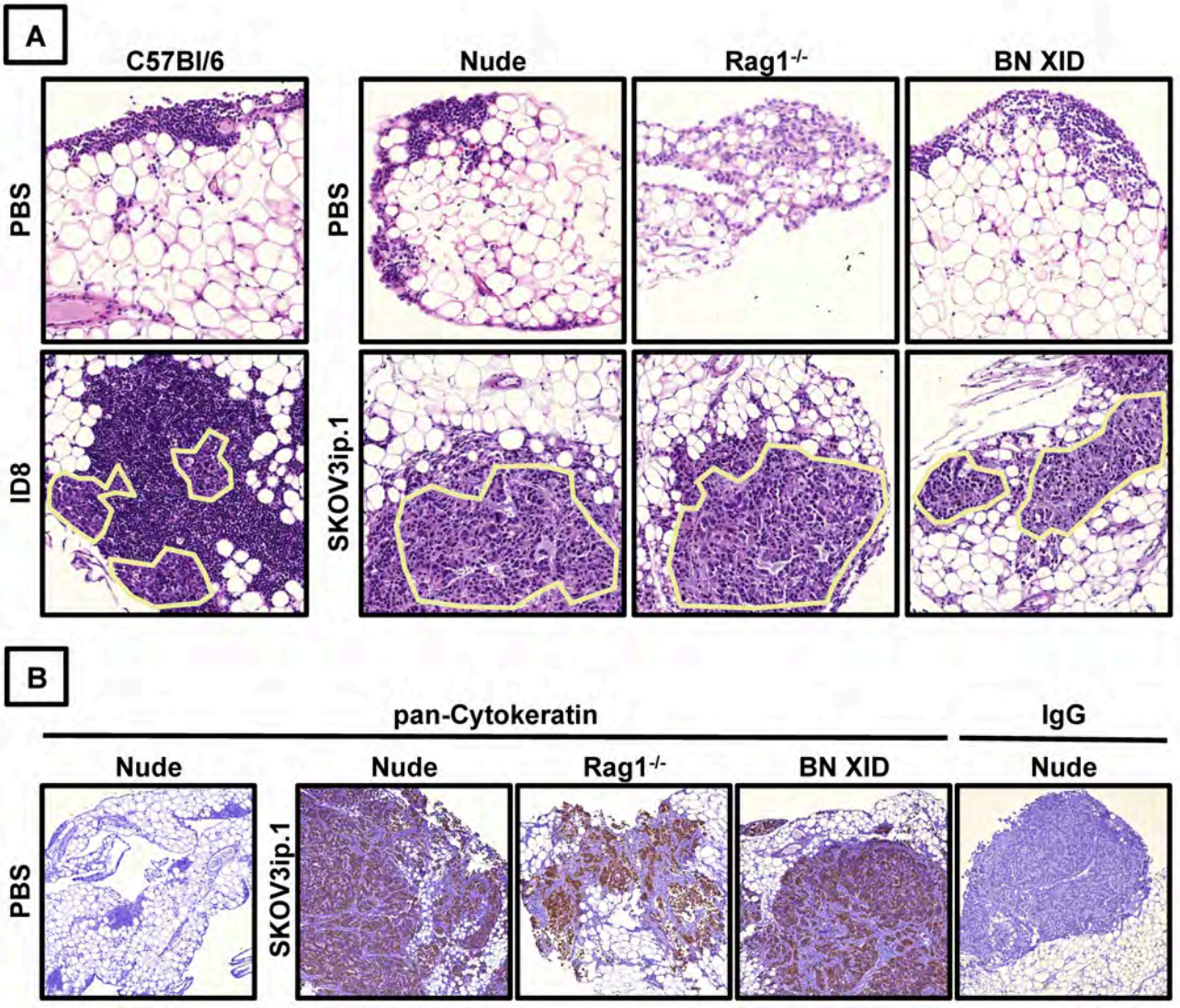

Clark and Krishnan, *et al*. Figure 7